Geochemical Journal, Vol. 50, pp. 493 to 525, 2016 doi:10.2343/geochemj.2.0449

Geochemical characteristics of hydrothermal fluids at Hatoma Knoll in the southern Okinawa Trough

Tomohiro Toki,[1]* Michihiro Itoh,[1] Daigo Iwata,[1] Shogo Ohshima,[1] Ryuichi Shinjo,[2] Jun-ichiro Ishibashi,[3] Urumu Tsunogai,[4†] Naoto Takahata,[5] Yuji Sano,[5] Toshiro Yamanaka,[6] Akira Ijiri,[7] Nobuaki Okabe,[8‡] Toshitaka Gamo,[8] Yasuyuki Muramatsu,[9] Yuichiro Ueno,[10,11] Shinsuke Kawagucci[10,12] and Ken Takai[10,12]

[1]Department of Chemistry, Biology and Marine Science, Faculty of Science, University of the Ryukyus, 1 Senbaru, Nishihara, Okinawa 903-0213, Japan
[2]Department of Physics and Earth Sciences, Faculty of Science, University of the Ryukyus, 1 Senbaru, Nishihara, Okinawa 903-0213, Japan
[3]Department of Earth and Planetary Sciences, Graduate School of Sciences, Kyushu University, 6-10-1 Hakozaki, Fukuoka 812-8581, Japan
[4]Earth and Planetary System Science, Faculty of Science, Hokkaido University, N10 W8 Kita-ku, Sapporo, Hokkaido 060-0810, Japan
[5]Marine Analytical Chemistry, Department of Chemical Oceanography, Atmosphere and Ocean Research Institute, The University of Tokyo, 5-1-5 Kashiwanoha, Kashiwa-shi, Chiba 277-8564, Japan
[6]Graduate School of Natural Science and Technology, Okayama University, 1-1 Naka 3-chome, Tsushima, Kita-ku, Okayama 700-8530, Japan
[7]Kochi Institute for Core Sample Research, Japan Agency for Marine-Earth Science and Technology (JAMSTEC), B200 Monobe, Nankoku 783-8502, Japan
[8]Marine Inorganic Chemistry Group, Department of Chemical Oceanography, Atmosphere and Ocean Research Institute, The University of Tokyo, 5-1-5 Kashiwanoha, Kashiwa-shi, Chiba 277-8564, Japan
[9]Department of Chemistry, Gakushuin University, 1-5-1 Mejiro, Toshima-ku, Tokyo 171-8588, Japan
[10]Precambrian Ecosystem Laboratory (PEL), Japan Agency for Marine-Earth Science and Technology (JAMSTEC), 2-15 Natsushima-cho, Yokosuka 237-0061, Japan
[11]Global Edge Institute, Tokyo Institute of Technology, G1-25 Nagatsuta, Midori-ku, Yokohama 226-8502, Japan
[12]Subsurface Geobiology Advanced Research (SUGAR) Project, Japan Agency for Marine-Earth Science and Technology (JAMSTEC), 2-15 Natsushima-cho, Yokosuka 237-0061, Japan

(*Received March 1, 2015; Accepted September 16, 2016*)

Chemical and isotopic compositions of hydrothermal fluids from Hatoma Knoll in the southern Okinawa Trough were investigated. The hydrothermal fluids were derived from a single pure hydrothermal fluid source, but they underwent phase separation beneath the seafloor prior to venting. Only vapor-like fluids vent at the Hatoma system, and the most active area is around the center of the crater, based on the location of the maximum temperature and the lowest Cl^- concentrations. Compared with other hydrothermal systems in the world, at Hatoma the pH and alkalinity, as well as the B, NH_4^+, K, Li, CO_2, and CH_4 concentrations, were higher, and the Fe and Al concentrations were lower, suggesting that the characteristics of the Hatoma hydrothermal fluids are comparable to those of the other Okinawa Trough hydrothermal fluids. Helium isotope ratios were lower than those of sediment-starved hydrothermal systems, suggesting that ^4He derived from the sediment is supplied to the hydrothermal fluids in Hatoma Knoll. The carbon isotope ratios of CO_2 in the hydrothermal fluids indicate an influence of organic carbon decomposition. The carbon isotope ratios of CH_4 in the hydrothermal fluids imply that most of the CH_4 originated from microbial methane produced in a recharge zone of the hydrothermal system. Although sediment influences are a typical feature of Okinawan Trough hydrothermal fluids, the Hatoma hydrothermal system has the lowest carbon isotope ratios of CH_4 among them, which suggests that Hatoma is the most

*Corresponding author (e-mail: toki@sci.u-ryukyu.ac.jp)

†Present address: Graduate School of Environmental Studies, Nagoya University, D2-1(510) Furo-cho, Chikusa-ku, Nagoya 464-8601, Japan.

‡Present address: Department of Chemistry, Gakushuin University, 1-5-1 Mejiro, Toshima-ku, Tokyo 171-8588, Japan.

highly influenced by the sediments in the recharge zone. Thus, the degree of the sediment influences has a variable in each hydrothermal field in the Okinawa Trough.

Keywords: hydrothermal fluid, Hatoma Knoll, Okinawa Trough, phase separation, sediment, subducting material

Introduction

Chemical and isotopic compositions of hydrothermal fluids can provide information about the sources of their chemical components and processes occurring during hydrothermal circulation beneath the seafloor in the hydrothermal system (Von Damm, 1995). In the Okinawa Trough, the hydrothermal systems are sediment-covered and have unique features that are different from those in sediment-starved mid-ocean ridges (MORs). The chemical composition of hydrothermal fluids from Okinawa Trough showed high-pH, and high concentrations of NH_4^+, boron (B), and iodine (I) relative to those of hydrothermal fluids from mid-ocean ridges, indicating the influence of terrigenous sediment covering Okinawa Trough (You *et al*., 1994). Furthermore, when compared with those from mid-ocean ridges, K and Li concentrations were high, suggesting the influence of acidic rocks (Sakai *et al*., 1990b). Moreover, in the most of the hydrothermal systems, phase separation would occur, and hydrothermal fluids of low-Cl^- concentrations have mainly been detected (e.g., Kawagucci, 2015). In this study, we collected hydrothermal fluids from the hydrothermal system of Hatoma Knoll in the southern Okinawa Trough and measured their chemical and isotopic compositions. In this paper, we describe the differences and affinities between Hatoma hydrothermal fluids and other hydrothermal fluids in the Okinawa Trough.

Geological Setting

The Okinawa Trough is a backarc basin that has developed where the Philippine Sea plate is subducting beneath the Eurasian plate (Fig. 1a; Lee *et al*., 1980). On the basis of water depth and the locations of gaps, the Okinawa Trough has been classified into three parts: north, middle, and south (Fig. 1b). The northern part of the Okinawa Trough (NOT) is characterized by volcanic activity and includes numerous presently active volcanic islands (Fig. 1b; Satsuma Iwo-jima Island at 30°47′ N, 130°18′ E and the Tokara Islands). Iheya North Knoll and Izena Hole in the middle Okinawa Trough (MOT) are in the backarc area of these volcanic islands (Fig. 1b). The volcanic activities southward from Iwotori Island cannot be traced by presently active volcanic islands, although old (Miocene and Pliocene) lavas have been found on Kume Island (Fig. 1b; Nakagawa and Murakami, 1975). Hatoma Knoll is about 10 km northwest of Daiichi and Daini Kohama Knolls and Iriomote Knoll corresponding to the southern extension of the arc system (Watanabe, 2000). The southern part of the backarc system is observed only as grabens in the deepest part of the Southern Okinawa Trough (SOT), but no rifting activity is actively occurring at present (Matsumoto *et al*., 2001).

Terrigenous sediments from the Eurasian continent cover the seafloor of the trough with a thickness of about 3 km in the SOT area, compared with more than 5 km in the MOT and up to 8 km in the NOT areas (Sibuet *et al*., 1987). These sediments are derived from Eurasian Continent or Taiwan (Dou *et al*., 2010a). During ODP Leg 195, Site 1202 was drilled off Taiwan at the depth of 1274 m corresponding to the SOT area, confirming the presence of sediments up to 410 m below the seafloor (Shipboard Scientific Party, 2002). A previous seismic data showed a thickness of 3.4 km of sediment on basalt in the southern Okinawa Trough (Lee *et al*., 1980). The Shimajiri Formation, which is 1.3 km thick, overlies the 2.1-km-thick Yaeyama Formation. The Shimajiri Formation is composed of Pliocene turbidites, clays, and ashes from the adjacent land area at that time (Natori, 1976; Suzuki and Sato, 1977). The Yaeyama Formation is composed of Miocene sand and mud (Hanzawa, 1935). Both these sedimentary rock formations are rich in organic matter (Motojima and Makino, 1965; Tsuburaya and Sato, 1985). A layer of basalt about 3.2 km thick underlies these two formations and overlies the continental crust, which is about 7.0 km thick (Lee *et al*., 1980). Composition of sediment in the middle Okinawa Trough is, based on cores of IMAGES, biogenic carbonate (15–25%; Chang *et al*., 2005) and biogenic opal (1.5–4%; Chang *et al*., 2009; Dou *et al*., 2010b). Besides, sediment without inorganic carbon and organic carbon is clay (20–30%), of which major components are illite of 70–80%, followed by smectite of 5–10% (Dou *et al*., 2010b). A main source of sediment for Okinawa Trough is the Yangtze River, and the debris derived from continental crust without organic and inorganic carbons is accounted for illite about 60–70% (e.g., Xu *et al*., 2014). On the other hand, sediment in the southern Okinawa Trough, based on Site 1202 during ODP Leg 195, contains carbonate of average 6.84% (Chang *et al*., 2005). Composition of sediment without inorganic and organic carbons is clay of 30–50%, of which 60–70% is illite and 5–10% is smectite (Diekmann *et al*., 2008). A content of biogenic opal could not been found, but a previous study via a sediment trap in the southern Okinawa Trough reported sediment contained carbonate and opal

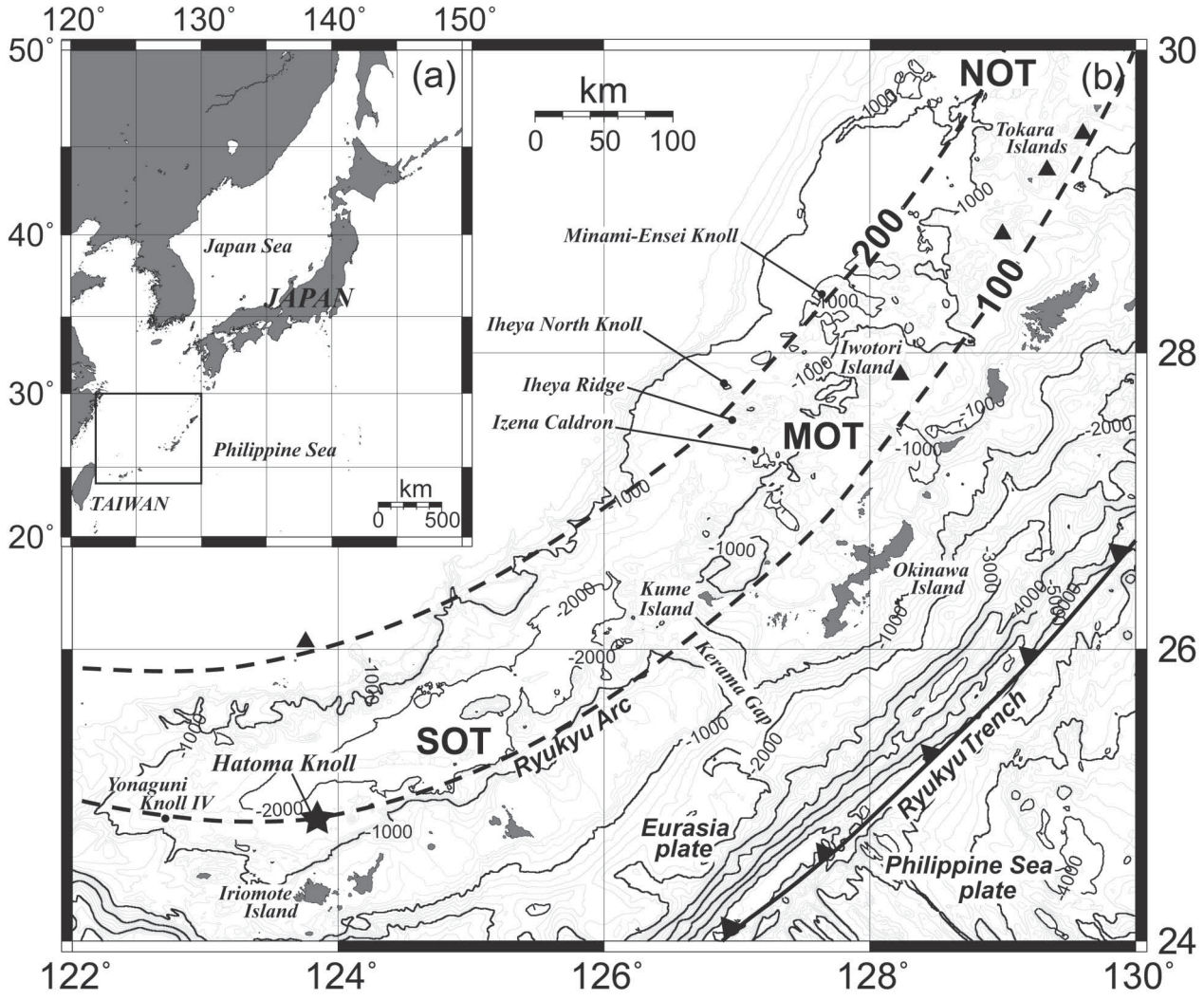

Fig. 1. (a) Map showing the location of the Okinawa Trough. The box indicates the area shown in panel b. (b) Location of Hatoma Knoll (star) and other known active hydrothermal fields (solid circles) in the Southern Okinawa Trough. Solid triangles indicate Quaternary volcanoes. The bathymetric contour intervals are 200 m (thin lines) and 1000 m (thick lines). Dashed lines represent the depth contours (100 and 200 km) of the Wadati-Benioff zone (Letouzey and Kimura, 1986; Pezzopane and Wesnousky, 1989). MOT and SOT indicate the Middle Okinawa Trough and the Southern Okinawa Trough, respectively. (c) Bathymetric map of Hatoma Knoll (100 m contour interval). The box indicates the area shown in panel d. (d) Bathymetry of the Hatoma hydrothermal field (10 m contour interval). Sampled vents discharging high-temperature fluids are denoted by triangles, and a vent discharging low-temperature fluids, shimmering, is denoted by a circle.

of several percent each (Hung *et al*., 2003).

Volcanic rocks from Hatoma Knoll have been classified as andesite to rhyolite by their chemical compositions (Watanabe, 1999). Basalts and dacite samples have also been collected from Hatoma Knoll (GANSEKI, 2007.10.22), and the basalts are not the same as mid-ocean ridge basalt (MORB), based on their Sr isotopic ratios and incompatible trace element compositions (Shinjo *et al*., 1999). Moreover, the SOT is characterized by a diversity of volcanic rocks (Shinjo *et al*., 1999; Watanabe, 2000). Shinjo *et al*. (1999) reported that volcanic rocks in the SOT are bimodally distributed, with a basalt peak and a rhyolite peak. Basalts and basaltic andesite have been sampled from both Daiichi and Daini Kohama Knolls, which are about 10 km from Hatoma Knoll, and rhyolites have been sampled from Iriomote Knoll, which is 30 km from Hatoma Knoll (Watanabe, 2000). Watanabe (2000) proposed that these four knolls are the present volcanic front, and pointed out that magma in the SOT is known to have a heterogeneous chemical composition. Shinjo and Kato (2000) proposed that the heterogeneous magma reflects the occurrence of fractionation below the

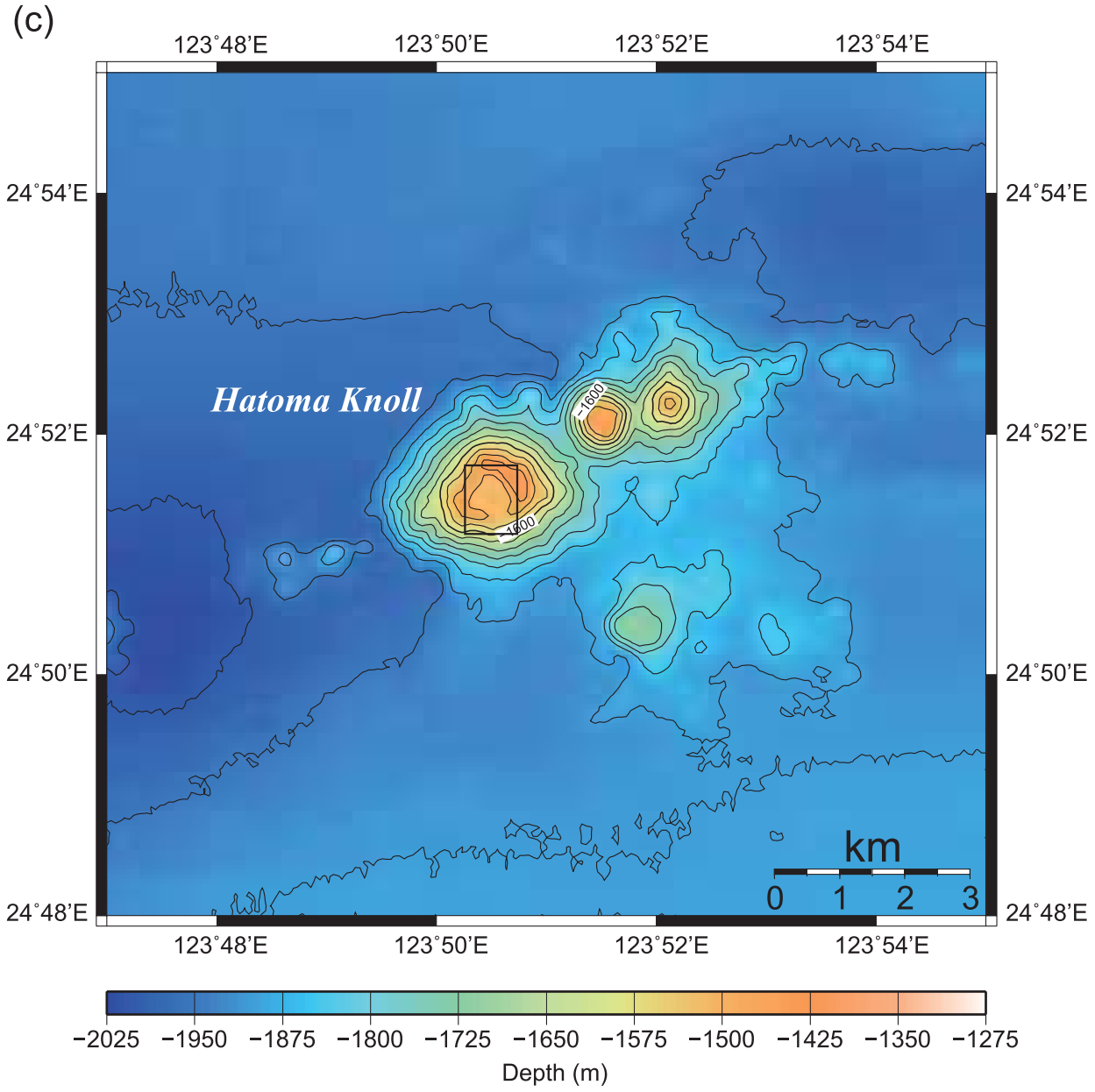

Fig. 1. (continued).

seafloor during magma formation.

Hatoma Knoll is in the SOT at 24°51′ N, 123°50′ E, about 48 km north of Iriomote Island (Fig. 1b). Its summit is about 500 m above the seafloor of the Okinawa Trough (1900 m below sea level), and the diameter at its base is about 4 km (Fig. 1c). On the top of Hatoma Knoll is a south-opening crater with a diameter of about 800 m and a wall about 150 m high (Figs. 1c and 1d). A hydrothermal field with a diameter of about 400 m and an estimated area of 16800 m^2 has been discovered in the crater (Watanabe, 1999, 2001), and the field has several hydrothermal vent sites, called (in the Okinawan language) Gusuku (a castle), Oritori (welcome), Chura (beautiful), Iri (west), and Agari (east) (Watanabe, 2001; Fig. 1d and Table 1a). At the Gusuku site, there are several active hydrothermal vents: C1, C2, C3, and 189-1 (Fig. 1d and Table 1a).

Samples

The hydrothermal fluid samples used in this study were collected from the hydrothermal system on Hatoma Knoll by the manned submersibles *Shinkai 2000* and *Shinkai 6500* and the remotely operated vehicle *Hyper Dolphin*

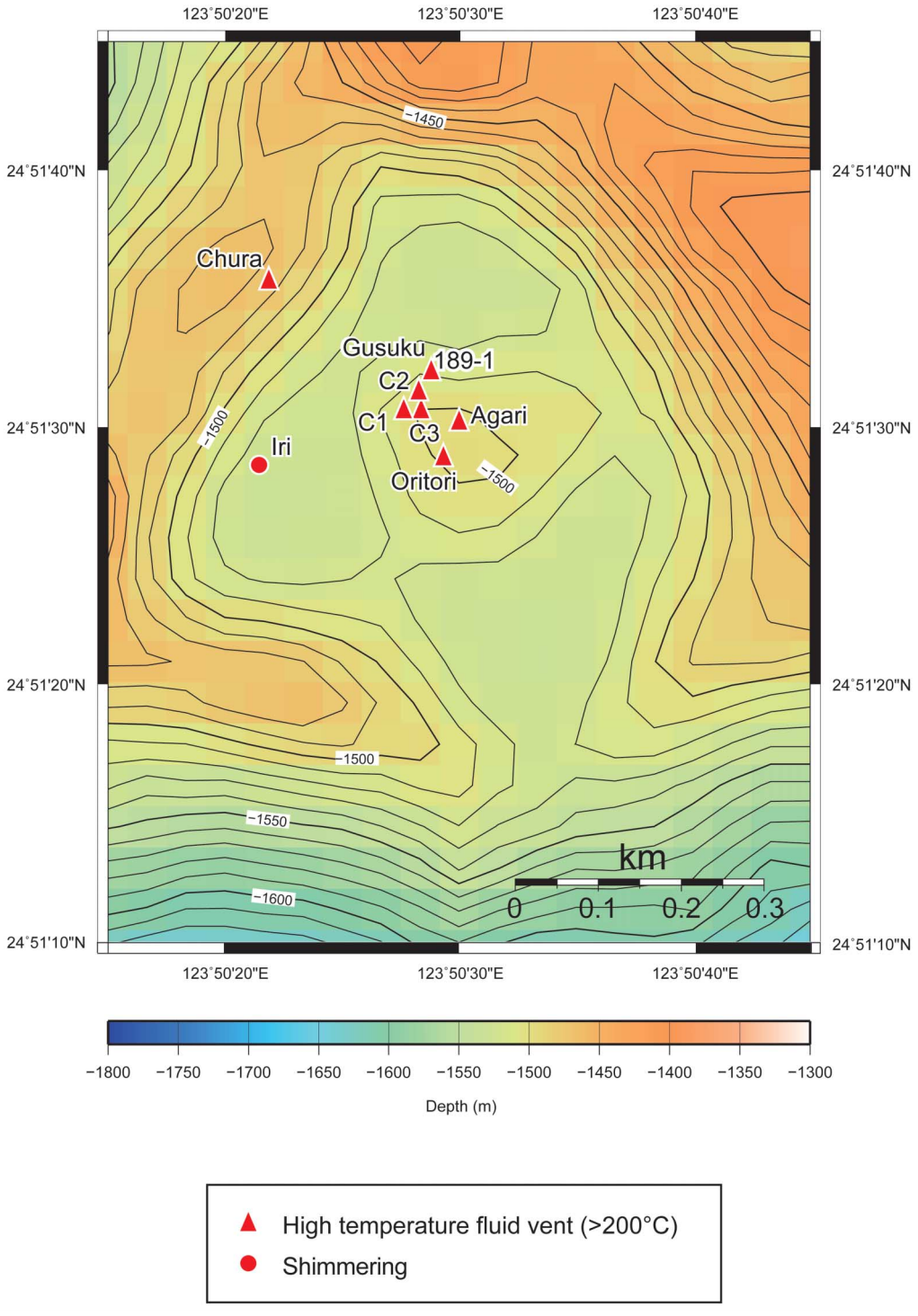

Fig. 1. (continued).

between 2000 and 2009 (Table 1a). The devices used to sample the fluids were a Water and Hydrothermal-fluid *Atsuryoku* gas-Tight Sampler (WHATS) (Saegusa *et al.*, 2006; Tsunogai *et al.*, 2003), a Cheap-WHATS (C-WHATS), a Vacuum sampler, and a titanium syringe-style 'major' sampler (Von Damm *et al.*, 1985b) for hydrothermal fluids, and a Niskin sampler for bottom seawater. C-WHATS samples use a system the same as WHATS, but the valves of its sampler bottles were manually closed using the manipulators of the submersibles contrary to

Table 1(a). Measured compositions of vent fluid samples from the Hatoma Knoll vent field for aqueous species

Site	Marker	Cruise	Dive	Sample	Description	Depth m	Latitude	Longitude	T_{max} ℃	pH	Alkalinity meq./L	Mg mmol/kg	Na mmol/kg
Oritori		NT00-06	2K1181	R1	Clear smoker	1,506	24°51.212′ N	123°50.578′ E	130	5.1	2.5	44.1	397
				R2	Clear smoker	1,506	24°51.212′ N	123°50.578′ E				42.6	403
				R3	Clear smoker	1,506	24°51.212′ N	123°50.578′ E					
				R4	Clear smoker	1,506	24°51.212′ N	123°50.578′ E		5.0	2.8	44.5	416
			2K1185	S	Clear smoker	1,490	24°51.210′ N	123°50.567′ E	259	5.2	3.3	35.9	375
			2K1186	R5	Clear smoker	1,516	24°51.216′ N	123°50.567′ E	195	5.0	2.3		
				R6	Clear smoker	1,491	24°51.216′ N	123°50.567′ E			4.3	3.3	297
				R7	Clear smoker	1,491	24°51.216′ N	123°50.567′ E					
			2K1187	R1	Clear smoker	1,493	24°51.216′ N	123°50.567′ E	180	6.7	2.3	53.3	429
				R2	Clear smoker	1,493	24°51.216′ N	123°50.567′ E		5.9	2.3	53.1	436
			2K1189	S	Clear smoker	1,493	24°51.216′ N	123°50.570′ E	301	5.0	2.7	47.6	403
Agari		NT00-06	2K1186	R1	Clear smoker	1,473	24°51.245′ N	123°50.602′ E	236	5.1	3.8	24.6	349
				R2	Clear smoker	1,473	24°51.245′ N	123°50.602′ E		5.2	4.9	1.6	291
				R3	Clear smoker	1,473	24°51.245′ N	123°50.602′ E					
				R4	Clear smoker	1,473	24°51.245′ N	123°50.602′ E		5.2	5.0	1.6	295
		NT08-13	3K869	V1	Clear smoker	1,478	24°51.480′ N	123°50.503′ E	301			0.8	281
				V2	Clear smoker	1,478	24°51.480′ N	123°50.503′ E			3.7	11.4	321
				B1	*Bathymodiolus*	1,479	24°51.480′ N	123°50.503′ E				51.8	457
			3K870	W3	*Bathymodiolus*	1,479	24°51.468′ N	123°50.515′ E	8	7.3	2.1	52.4	450
				W4	*Bathymodiolus*	1,479	24°51.468′ N	123°50.515′ E	9			48.6	424
			3K872	B1	*Bathymodiolus*	1,479	24°51.489′ N	123°50.504′ E		6.3	2.0	51.5	453
				W3	*Bathymodiolus*	1,479	24°51.489′ N	123°50.504′ E		6.0	2.0	51.0	455
				W4	*Bathymodiolus*	1,479	24°51.489′ N	123°50.504′ E				47.8	425
		NT09-11	3K1036	B1	*Bathymodiolus*	1,479	24°51.482′ N	123°50.505′ E		7.5	2.5	49.5	437
				W1	*Bathymodiolus*	1,479	24°51.482′ N	123°50.505′ E	4	7.4	2.4	49.9	438
				W2	*Bathymodiolus*	1,479	24°51.482′ N	123°50.505′ E	4				
Iri	184-1	NT07-12	3K709	W3	Clear smoker	1,532	24°51.464′ N	123°50.380′ E	75			26.4	367
				W4	Clear smoker	1,532	24°51.464′ N	123°50.380′ E	70	5.7	5.5	31.0	388
Chura		NT00-06	2K1187	R3	Clear smoker	1,516	24°51.269′ N	123°50.481′ E	160	7.0	2.4	52.7	435
				R4	Clear smoker	1,516	24°51.269′ N	123°50.481′ E		6.6	2.4	54.2	423
				R5	Clear smoker	1,516	24°51.269′ N	123°50.481′ E		5.0	2.3	53.9	429
				R6	Clear smoker	1,491	24°51.296′ N	123°50.458′ E		5.5	2.9	39.1	389
				R7	Clear smoker	1,491	24°51.296′ N	123°50.458′ E		7.6	2.4	53.7	423
		NT08-13	3K871	B1	Galatheidae	1,507	24°51.592′ N	123°50.400′ E		6.7	1.9		
				W1	Clear smoker	1,504	24°51.594′ N	123°50.392′ E	206			18.4	345
				W2	Clear smoker	1,504	24°51.594′ N	123°50.392′ E	226			20.4	332
				W3	Clear smoker	1,504	24°51.594′ N	123°50.392′ E	178			32.3	369
				W4	Clear smoker	1,504	24°51.594′ N	123°50.392′ E	131			37.4	392
Reference		NT00-06	2K1184	N	Bottom seawater	1,523	24°51.229′ N	123°50.458′ E		7.6	2.3	54.1	432
			2K1185	N	Bottom seawater	1,520	24°51.222′ N	123°50.466′ E		7.6	2.4	54.1	440
			2K1186	N	Bottom seawater	1,493	24°51.216′ N	123°50.567′ E		7.5	2.4	53.8	442
			2K1189	N	Bottom seawater	1,451	24°51.255′ N	123°50.567′ E		6.6	2.4	54.1	428
		YK07-04	6K999	N	Bottom seawater	1,505	24°51.559′ N	123°50.623′ E		7.4	1.2	46.6	436
			6K1000	N	Bottom seawater	1,473	24°51.522′ N	123°50.471′ E		7.2	2.4	48.4	445
		NT07-12	3K707	V1	Bottom seawater	1,527	24°51.564′ N	123°50.387′ E				49.8	437
				V2	Bottom seawater	1,527	24°51.564′ N	123°50.387′ E		7.4	2.2	52.8	457
		NT08-13	3K871	V1	Bottom seawater	1,452	24°51.609′ N	123°50.350′ E		7.5	1.6	52.8	454
		NT09-11	3K1035	N2	Bottom seawater	1,471	24°51.511′ N	123°50.473′ E		6.8	2.6	49.3	435
			3K1039	N1	Bottom seawater	1,472	24°51.495′ N	123°50.460′ E		7.4		49.9	423
				N2	Bottom seawater	1,450	24°51.485′ N	123°50.479′ E		7.5		49.8	429

WHATS. Vacuum sampler, which was made by reference to Lupton *et al*. (2008), used the same gas-tight bottles as WHATS, and a nozzle was directly attached to each bottle with a gas-tight valve. And before the dive, the air in the bottle was pumped out to a vacuum and the valve was closed; then during the dive, the nozzle was placed into the vent being sampled and the sampler valve was opened by a manipulator of a submersible. Venting fluids were

Table 1(a). (continued)

Site	K mmol/kg	Li mmol/kg	Cl^- mmol/kg	SO_4^{2-} mmol/kg	Si mmol/kg	Ca mmol/kg	Sr μmol/kg	Ba mmol/kg	Mn μmol/kg	Fe nmol/kg	I μmol/kg	NH_4^+ mmol/L	B mmol/kg	Al nmol/kg
Oritori	16.2		489	21.9	2.37	9.9	83.8					1.00	0.76	
	18.3		488	21.3	2.86	10.4	84.9					1.38	0.90	
	17.7		498	21.9	2.67	10.2	85.6					1.25	0.88	
	24.4		499	27.5	4.04	10.8	79.7		107			2.37	2.37	
	52.5		387	2.1	11.93	14.3	64.9		460			7.12	2.88	
	9.9		527	26.7	0.38	9.4	88.6					0.10	0.38	
	9.7		548	27.3	0.14	9.3	89.8						0.36	
	14.2		537	24.9	1.43	9.8	87.3					0.77	1.24	
Agari	33.7		438	12.2	7.25	12.3	74.6		260			3.41	1.81	
	53.5		382	1.7	12.50	14.4	64.1		473			6.77	2.99	
	53.3		377	1.2	12.39	14.4	64.5		472			6.34	2.97	
	53.3	1.87			12.31	16.8	68.1	2.6	539	322			2.94	
	46.9	1.67	425	7.4	8.92	15.3	70.0	9.8	415	38	62.7	4.76	2.49	2959
	10.1		524	26.9	0.13	10.2	90.5				1.1	0.00	0.43	73
	9.9		542	26.7	0.13	10.1	88.2				1.5	0.01	0.39	33
	9.3					9.7	83.8	2.1	9	86			0.38	
	9.9		522	26.5	0.13	10.2	89.9				1.2	0.02	0.41	48
	10.0		535	26.4	0.14	10.2	89.3				1.3	0.03	0.41	148
	9.5					9.5	83.7		10	101			0.39	
	9.7		539	27.7	0.13	9.8						0.00		
	9.8		519	27.3	0.13	9.9						0.01		
Iri	29.5	0.57			4.26	12.2	69.1	6.8	1858					
	28.1	0.51	479	16.9	3.02	12.1	71.2		165	51	30.0	2.68		
Chura	9.6		534	26.9	0.15	9.4	90.2						0.38	
	9.8		536	27.3	0.16	9.4	90.6						0.36	
	9.2		543	27.5	–0.10	9.5	90.3						0.36	
	21.9		497	19.7	3.31	10.5	83.4		117			1.68	1.08	
	10.1		541	27.0	0.34	9.5	91.1					0.15	0.40	
	39.7	1.35	435	9.8	7.77	13.4	71.6	33.7	408	59		4.26	1.99	3938
	34.6	1.24			6.99	12.5	69.8	49.2	341	70			1.74	
	24.2	0.96			4.27	11.3	76.2	48.9	232	98			1.16	
	19.5	0.76			2.87	11.0	79.1	11.5	161	114			0.91	
Reference	9.4		526	26.5	0.29	9.5	90.1						0.34	
	9.2		530		0.47	9.3	90.9						0.37	
	9.6		528	27.0	0.65	9.3	89.7						0.33	
	9.7		540	27.9	0.67	9.4	91.1						0.29	
	13.2	0.02	541	27.8	0.09	9.0	84.1		0	7	0.7		0.43	
	12.3	0.05	534	27.3	0.18	9.1	83.7		2	4	0.7		0.53	
	10.1	0.07			0.11	9.7	77.2			78				
	10.6	0.09	542	28.4	0.12	10.3	81.4			5	1.2			
	10.0		539	27.6	0.13	10.2	89.6				1.2	0.00	0.38	45
	9.3		538	27.6	0.10	9.6						0.00		
	9.0		534	28.8	0.13	9.8						0.00		
	8.8		533	28.9	0.13	9.8						0.00		

sucked into the bottle, and then the valve was closed by the manipulator until it was gas-tight. A titanium syringe-style 'major' sampler is used to sample hydrothermal fluids from the early period on a hydrothermal study (Von Damm *et al*., 1985b), which is like a syringe of titanium with a spring and trigger. After sampling, the sampler is opened on shipboard, and a precipitation in the sampler can be recovered, which has an advantage to measure

Table 1(b). Measured compositions of vent fluid samples from the Hatoma Knoll vent field for volatiles and isotopes

Site	Marker	Cruise	Dive	Sample	ΣCO_2 mmol/L	H_2S mmol/L	CH_4 mmol/L	H_2 μmol/L	C_2H_6 μmol/L	He μmol/L	C_3H_8 nmol/L	$\delta^{18}O(H_2O)$ ‰VSMOW
Oritori		NT00-06	2K1181	R1								
				R2								
				R3								
				R4								
			2K1185	S								
			2K1186	R5								
				R6								
				R7								
			2K1187	R1								
				R2								
			2K1189	S								
Agari		NT00-06	2K1186	R1								
				R2								
				R3								
				R4								
		NT08-13	3K869	V1	141		2.9	90	11.0			
				V2				162				1.38
				B1								−0.35
			3K870	W3		0.0						−0.40
				W4	3		0.0					
			3K872	B1								−0.30
				W3		0.2						−0.20
				W4	2		0.2	14				
		NT09-11	3K1036	B1		0.0						−0.43
				W1								−0.44
				W2	0		0.0	<0.01			<10	
Iri	184-1	NT07-12	3K709	W3	215		12.8	41	17.3			
				W4								0.65
Chura		NT00-06	2K1187	R3								
				R4								
				R5								
				R6								
				R7								
		NT08-13	3K871	B1		0.0						
				W1								1.19
				W2	97		3.4	53				
				W3				30				
				W4	4		0.0					
Reference		NT00-06	2K1184	N								
			2K1185	N								
			2K1186	N								
			2K1189	N								
		YK07-04	6K999	N		0.1						−0.45
			6K1000	N		0.1						−0.08
		NT07-12	3K707	V1	2		0.0	10				−0.11
				V2								
		NT08-13	3K871	V1		0.0						−0.23
		NT09-11	3K1035	N2		11.4						−0.45
			3K1039	N1		2.0						−0.36
				N2		N.D.						−0.44

Table 1(b). (continued)

Site	Marker	Cruise	Dive	Sample	$\delta D(H_2O)$ ‰VSMOW	$\delta^{13}C(CO_2)$ ‰VPDB	$\delta^{13}C(CH_4)$ ‰VPDB	$\delta^{13}C(C_2H_6)$ ‰VPDB	$^3He/^4He$ R_A	$^4He/^{20}Ne$
Oritori		NT00-06	2K1181	R1						
				R2						
				R3						
				R4					6.3	2.9
			2K1185	S						
			2K1186	R5						
				R6					6.9	4.1
				R7						
			2K1187	R1						
				R2					3.2	0.5
			2K1189	S						
Agari		NT00-06	2K1186	R1						
				R2						
				R3					5.8	1.7
				R4					3.2	0.6
		NT08-13	3K869	V1		−8.6	−50.5	−24.5	6.0	2.4
				V2	−2.09				7.0	23.3
				B1	−3.32					
			3K870	W3	−1.22					
				W4		−5.0	−45.2		2.1	0.4
			3K872	B1	1.11					
				W3	−2.02					
				W4		−19.0	−53.1		2.8	0.7
		NT09-11	3K1036	B1	1.78					
				W1	1.49					
				W2			−49.3		2.7	0.4
Iri	184-1	NT07-12	3K709	W3		−7.9	−54.5	−17.3		
				W4	−1.74					
Chura		NT00-06	2K1187	R3						
				R4						
				R5						
				R6					6.6	2.5
				R7					6.6	2.5
		NT08-13	3K871	B1						
				W1	−2.50					
				W2		−9.1	−50.1		5.2	1.4
				W3					2.4	0.5
				W4		−16.2	−51.7		0.4	1.1
Reference		NT00-06	2K1184	N					4.3	0.5
			2K1185	N						
			2K1186	N					2.4	0.3
			2K1189	N					3.1	0.6
		YK07-04	6K999	N	−0.42					
			6K1000	N	−1.94					
		NT07-12	3K707	V1	−1.37	−3.9	−50.1		1.6	0.3
				V2						
		NT08-13	3K871	V1	0.38					
		NT09-11	3K1035	N2	2.64					
			3K1039	N1	2.34					
				N2	−2.52					

concentrations of metals in precise (Metz and Trefry, 2000). The locations of the sampling sites, the samplers used at each site, the features of the hydrothermal vents, and the maximum temperature of the hydrothermal fluids are listed in Table 1a. Dive numbers 2K1181–1189 were performed in 2000, and dive number 6K999–1001 was performed in March 2007, 3K705–709 in July 2007, 3K866–873 in 2008, and 3K1035–1039 in 2009 (Table 1a).

These fluid samples were taken in duplicate if possible for gas and water chemistry of dissolved components. The bottles of hydrothermal fluid for gas chemistry collected by WHATS, C-WHATS, and Vacuum sampler were connected to a vacuum line as soon as possible after their recovery for dissolved gas extraction; then the fluid in the sample bottle was introduced into an evacuated container containing sulfamic acid and mercury chloride to precipitate hydrogen sulfide from the fluid as mercury sulfide (Konno *et al*., 2006). A magnetic stirrer was used to mix the fluid in the container enough to cause degassing of dissolved gases from the fluid and to reach equilibrium between the gas phase and the liquid phase in the container. The gas phase was then expanded into a 50 cm^3 evacuated stainless steel sample canister, the inside pressure was measured, and then the canister was sealed for preservation. Chemical and isotopic compositions of the gas in the canister were measured in on-land laboratories. The residual liquid in the container was analyzed for major chemical components in an on-land laboratory.

In the case of the bottles of hydrothermal fluid for water chemistry, 20 cm^3 of the unfiltered collected sample was first transferred into two vials, each with a volume of 10 cm^3, for measurement of the hydrogen sulfide concentration (where the samples were inevitably degassed, and the H_2S data correspond to the minimum value for each sample), pH, and alkalinity, and the remaining fluid was filtered through a disposable syringe filter (pore size: 0.45 μm, ADVANTEC, Mixed Cellulose Ester, non-sterile). Then, 15 cm^3 and 30 cm^3 of the filtered fluid were transferred to a polyethylene bottle, respectively, and 30 cm^3 of them was acidified with 0.3 cm^3 of 3N HNO_3 to lower the pH to less than 2 for cation analyses in the on-land laboratories. On the other hand, 15 cm^3 of them was used for measurement of Si and ammonium concentrations onboard ship within several hours of collection, and the rest fluid of 15 cm^3 after onboard measurements was preserved in a refrigerator for later anion analyses and isotope analyses on land.

Analyses

The pH was determined by pH meter and alkalinity was determined by the Gran plot method (Gieskes *et al*., 1991) at precisions of 0.02 units and 5%, respectively. The H_2S concentration was determined by the methylene-blue method (Cline, 1969), with a precision of 10%. The Si concentration was analyzed by the molybdate-blue method (Gieskes *et al*., 1991) with 2% precision. The NH_4^+ concentration was measured by the Indo-phenol method (Gieskes *et al*., 1991), with a precision of 7%. The K concentration was measured by Zeeman Atomic Adsorption Spectrometry with 4% precision. The Ca, Mg, and Na concentrations were measured by inductively coupled plasma atomic emission spectrometry, with precisions within 2%. The Cl^- concentration was measured by the Mohr method (Gieskes *et al*., 1991), with a precision of 0.3%. The SO_4^{2-} concentration was measured by ion chromatography with a precision of 4%. The I concentration was determined by induced coupled plasma mass spectrometry with a precision of 5% (Muramatsu *et al*., 2007). The Al concentration was determined by fluorometry using Lumogallion with a precision of 2.7% (Obata *et al*., 2000).

The concentrations and carbon isotopic ratios of $\sum CO_2$ (sum of CO_2, H_2CO_3, HCO_3^-, and CO_3^{2-}), CH_4, and C_2H_6 were analyzed by a continuous flow stable isotope mass spectrometry system (Finnigan MAT252); the precision for concentration was 6.5% and that for the isotope ratio was 0.3‰ (Tsunogai *et al*., 2000). Concentrations of He and H_2 were determined with a gas chromatograph (GC7000TF; J-Science Lab. Co., Ltd.) equipped with a thermal conductivity detector. The precision was 4% for He and 3% for H_2. The hydrogen isotopic ratio of water of the liquid samples was measured with a mass spectrometer (VG SIRA10; V-G Isogas Ltd.) equipped with a Cr reactor (Itai and Kusakabe, 2004) at a precision of 0.5‰, which is a simple method using metal chromium for a reductant, not the H_2-H_2O equilibration method too hard to strictly control temperature (Coplen *et al*., 1991). The oxygen isotopic ratio of water of the liquid samples was measured by mass spectrometer after equilibration of an aliquot of the liquid sample with CO_2 gas (Epstein and Mayeda, 1953); the measurement precision was 0.1‰. For the isotope of interest, X, δX is defined by the following expression:

$$\delta X\ (‰) = ((R_{samp} - R_{std})/R_{std}) \times 1000, \qquad (1)$$

where R_{samp} and R_{std} are the isotope ratios of the sample and standard, respectively. $\delta^{13}C(CO_2)$ and $\delta^{13}C(CH_4)$ values are expressed relative to the VPDB scale, whereas $\delta^{18}O$ and δD values are both expressed relative to VSMOW. The isotopic ratio of He ($^3He/^4He$) and the ratio of He to Ne ($^4He/^{20}Ne$) were measured with a noble gas mass spectrometer (VG5400; V-G Isogas Ltd.; Sano and Wakita, 1988) with precisions of 1.1% and 10%, respectively. The $^3He/^4He$ ratios are presented relative to the atmospheric value, R/R_A, where R_A is the atmospheric $^3He/^4He$ ratio: 1.39×10^{-6}.

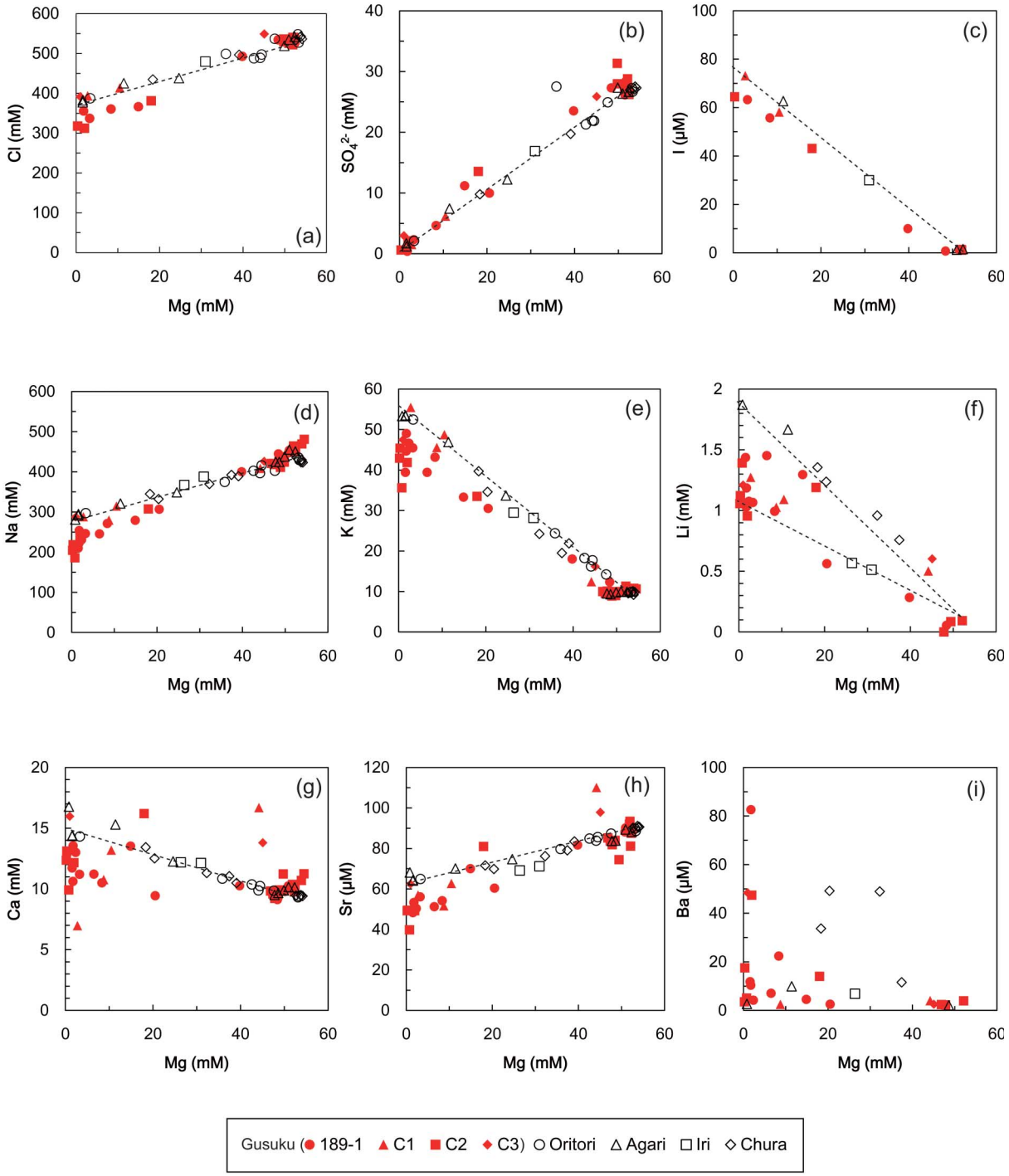

Fig. 2. Relationships between the concentration of measured chemical components and the Mg concentration in vent water samples collected for this study from eight vents of the hydrothermal Hatoma field: (a) Cl^-, (b) SO_4^{2-}, (c) I, (d) Na, (e) K, (f) Li, (g) Ca, (h) Sr, and (i) Ba.

Results and Discussion

End-members of the Hatoma hydrothermal fluids

The analytical results for vent fluids from Hatoma Knoll are shown in Table 1a for fluid chemistry, together with the maximum temperatures recorded during sampling, and Table 1b for gas chemistry. Generally, during the hydrothermal circulation, hydrothermal fluids reacted

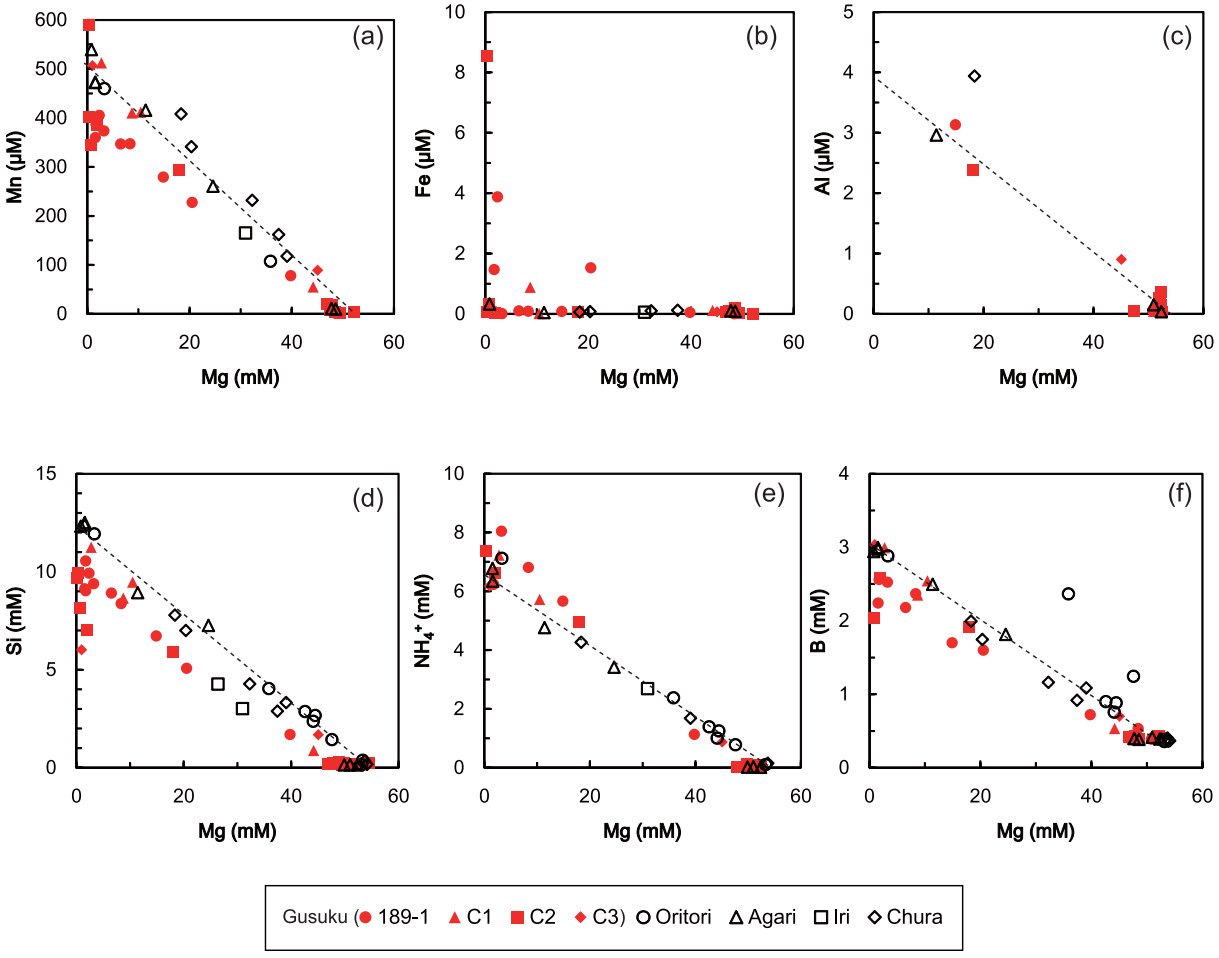

Fig. 3. Relationships between the concentration of measured chemical components and the Mg concentration in vent water samples collected for this study from eight vents of the hydrothermal Hatoma field: (a) Mn, (b) Fe, (c) Al, (d) Si, (e) NH_4^+, and (f) B.

with rocks beneath the seafloor and then became mixed with seawater prior to being vented from the seafloor (e.g., Von Damm, 1995). In fact, we need to verify whether we can apply the scenario to the Hatoma hydrothermal system. For the purpose, we use a "Mg-diagram" (Von Damm *et al.*, 1985b). In this diagram, we use the fact that experimental hydrothermal fluids are low-Mg relative to that of seawater (Bischoff and Dickson, 1975; Hajash and Chandler, 1982; Mottl and Holland, 1978; Ogawa *et al.*, 2005; Seyfried Jr. and Bischoff, 1981; Shiraki *et al.*, 1987). When the pure hydrothermal fluid mixed with the seawater, we can find linear relationships in the Mg-diagram. We can estimate the compositions of the pure hydrothermal fluids as the y-axis intercepts of the diagram (Von Damm *et al.*, 1985b). We show the diagram in Figs. 2, 3, and 4, and the calculated end-member concentrations are shown in Table 2. But pH and alkalinity do not behave conservatively with seawater admixing, and we listed the pH and alkalinity values of the sample with the minimum Mg concentration in Table 2a. Table 2a shows the end-member compositions of dissolved elements along with the maximum temperature at each vent site, and Table 2b shows the end-member compositions of gaseous components at each site. The end-member values are also plotted on Fig. 5 relative to the Cl end-member values and compared with those of hydrothermal fluids from the East Pacific Rise (EPR) at 21°N as a representative of mid-ocean ridge systems (Von Damm *et al.*, 2002), the Lau and Manus Basins for a comparison to other backarc hydrothermal systems (Mottl *et al.*, 2011; Reeves *et al.*, 2011), Suiyo seamount and Kermadec arc for that to other arc hydrothermal systems (de Ronde *et al.*, 2011; Tsunogai *et al.*, 1994), Middle Valley and Guaymas Basin for that to other sedimented systems (Butterfield *et al.*, 1994a; Von Damm *et al.*, 1985a), and the Okinawa Trough (Minami-Ensei: Chiba *et al.*, 1993; Kawagucci *et al.*, 2013b, Iheya North: Kawagucci *et al.*, 2011, JADE: Ishibashi *et al.*, 1995, HAKUREI: Ishibashi *et al.*, 2014,

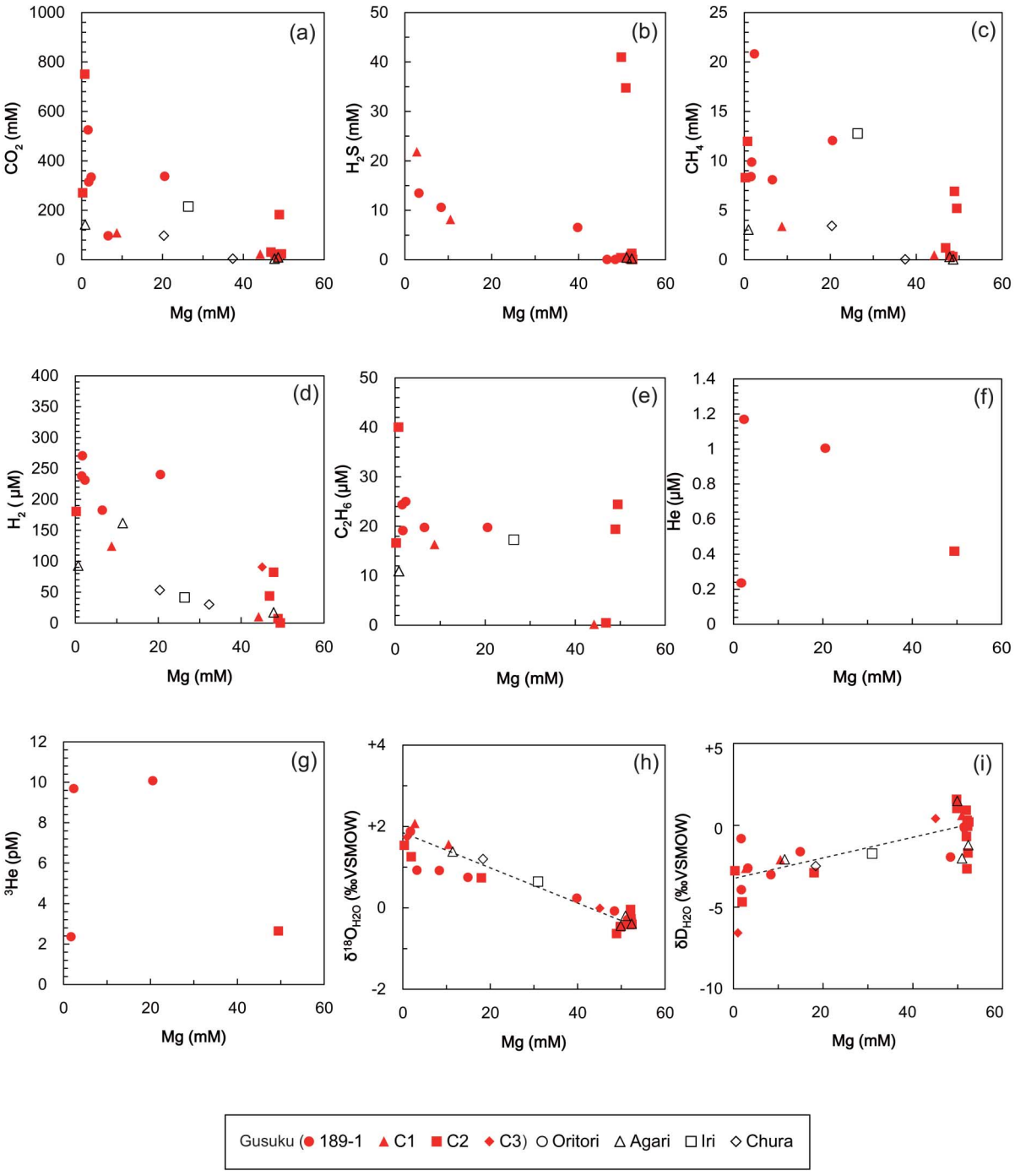

Fig. 4. Relationships between the concentration of measured chemical components and the Mg concentration in vent water samples collected for this study from eight vents of the hydrothermal Hatoma field: (a) CO_2, (b) H_2S, (c) CH_4, (d) H_2, (e) C_2H_6, (f) He, (g) ^3He, (h) $\delta^{18}O_{H2O}$, and (i) δD_{H2O}.

and Yonaguni IV: Konno *et al*., 2006; Suzuki *et al*., 2008).

Maximum temperature The highest temperature at each site ranged from 75°C to 325°C (Table 2a). The temperature was higher than 300°C at the Gusuku, Oritori, and Agari sites located around the center of the crater (Fig. 1d). At Gusuku, the venting showed a distinctive 'flame-like' discharge, which is usually seen when the hydrothermal fluids are boiling at the seafloor due to the vapor and brine phases being unable to segregate in the vent and making a very reflective 'flame' for the submersible

Table 2. End-member compositions of vent fluids from Hatoma Knoll

Site	T_{max}	pH*	Alk**	Na		K		Li		Cl^-		SO_4^{2-}	
			meq./L	mmol/kg		mmol/kg		mmol/kg		mmol/kg		mmol/kg	
Gusuku													
189-1	323	5.4	4.9	222	±6	46.0	±0.5	1.21	±0.02	331	±2	–0.56	±0.02
C1	322	5.4	2.8	270	±14	54.7	±1.0	1.43	±0.04	387	±3	0.05	±0.07
C2	325	5.4	4.7	205	±7	40.8	±0.6	1.23	±0.03	303	±2	0.48	±0.02
C3		5.2	5.6	287	±20	48.0	±1.3	1.52	±0.07	393	±4	2.50	±0.12
Oritori	301		4.3	285	±21	55.2	±1.2			379	±4	0.40	±0.10
Agari	301	5.2	4.9	285	±11	54.8	±0.8	2.07	±0.09	378	±2	0.59	±0.04
Iri	75	5.7	5.5	310	±41	50.9	±1.4	1.29	±0.06	428	±12	3.12	±1.77
Chura	226	5.5	2.9	283	±24	50.4	±1.0	2.36	±0.07	389	±6	0.44	±0.65

Site	Si		Ca		Sr		Mn		I		NH_4^+		B	
	mmol/kg		mmol/kg		μmol/kg		μmol/kg		μmol/kg		mmol/L		mmol/kg	
Gusuku														
189-1	9.78	±0.0	11.6	±0.2	49.5	±0.8	402	±7	62.5	±2.3	7.09	0.24	2.43	±0.03
C1	11.3	±0.1	8.8	±0.2	51.7	±1.3	529	±15	75.7	±2.7	7.42	±0.4	2.88	±0.05
C2	8.63	±0.0	11.4	±0.2	46.4	±0.8	417	±10	66.2	±2.3	7.42	±0.3	2.33	±0.04
C3	6.39	±0.1	16.0	±0.6	62.1	±2.2	580	±23			6.70	±0.4	2.94	±0.09
Oritori	13.0	±0.1	14.1	±0.5	63.1	±2.3	473	±20			8.16	±0.3	3.59	±0.07
Agari	12.5	±0.1	15.2	±0.3	64.6	±1.2	518	±12	82.0	±4.0	6.55	±0.2	3.03	±0.04
Iri	8.3	±0.1	14.5	±0.7	48.7	±3.9	537	±30	78.8	±4.3	6.96	±0.5	1.67	±0.15
Chura	11.6	±0.1	14.4	±0.5	59.7	±2.5	659	±19			7.02	±0.4	2.59	±0.05

Site	Al		NH_4^+		B		Al		ΣCO_2	H_2S	H_2	C_2H_6
	nmol/kg		mmol/L		mmol/kg		nmol/kg		mmol/L	mmol/L	μmol/L	μmol/L
Gusuku												
189-1	4392	±242	7.09	0.24	2.43	±0.03	4392	±242	525	13.5	271	25.0
C1			7.42	±0.4	2.88	±0.05			109	21.8	124	16.3
C2	3626	±206	7.42	±0.3	2.33	±0.04	3626	±206	1770	40.9	1228	40.0
C3			6.70	±0.4	2.94	±0.09			448		90	17.7
Oritori			8.16	±0.3	3.59	±0.07						
Agari	3774	±202	6.55	±0.2	3.03	±0.04	3774	±202	141		162	11.0
Iri			6.96	±0.5	1.67	±0.15			215		41	17.3
Chura	6015	±168	7.02	±0.4	2.59	±0.05	6015	±168	97		53	

Site	C_3H_8	He	$\delta^{18}O(H_2O)$		$\delta D(H_2O)$		$\delta^{13}C(CO_2)$		$\delta^{13}C(CH_4)$		$^3He/^4He_{corr}$	
	μmol/L	μmol/L	‰VSMOW		‰VSMOW		‰VPDB		‰VPDB		R_A	
Gusuku												
189-1		1.2	1.4	±0.05	–2.7	±0.5	–8.8	±0.4	–52.3	±2.43	7.2	±0.6
C1			2.2	±0.08	–2.8	±0.8	–9.5	±0.7	–53.1	±3.46	6.4	±0.3
C2		0.4	1.1	±0.07	–4.8	±0.6	–8.2	±0.4	–49.1	±1.05	6.8	±1.0
C3			1.8	±0.10	–6.7	±1.0					6.4	±0.3
Oritori											7.0	±0.6
Agari			1.9	±0.13	–2.4	±1.3	–9.6	±1.0	–49.5	±2.49	6.7	±0.5
Iri			2.1	±0.38	–4.8	±2.7	–8.0	±0.7	–54.5	±5.06		
Chura			2.0	±0.16	–4.0	±1.6	–12.9	±1.2	–50.9	±3.35	5.9	±0.6

**pH values were measured at 25°C.*
***Alk means Alkalinity.*

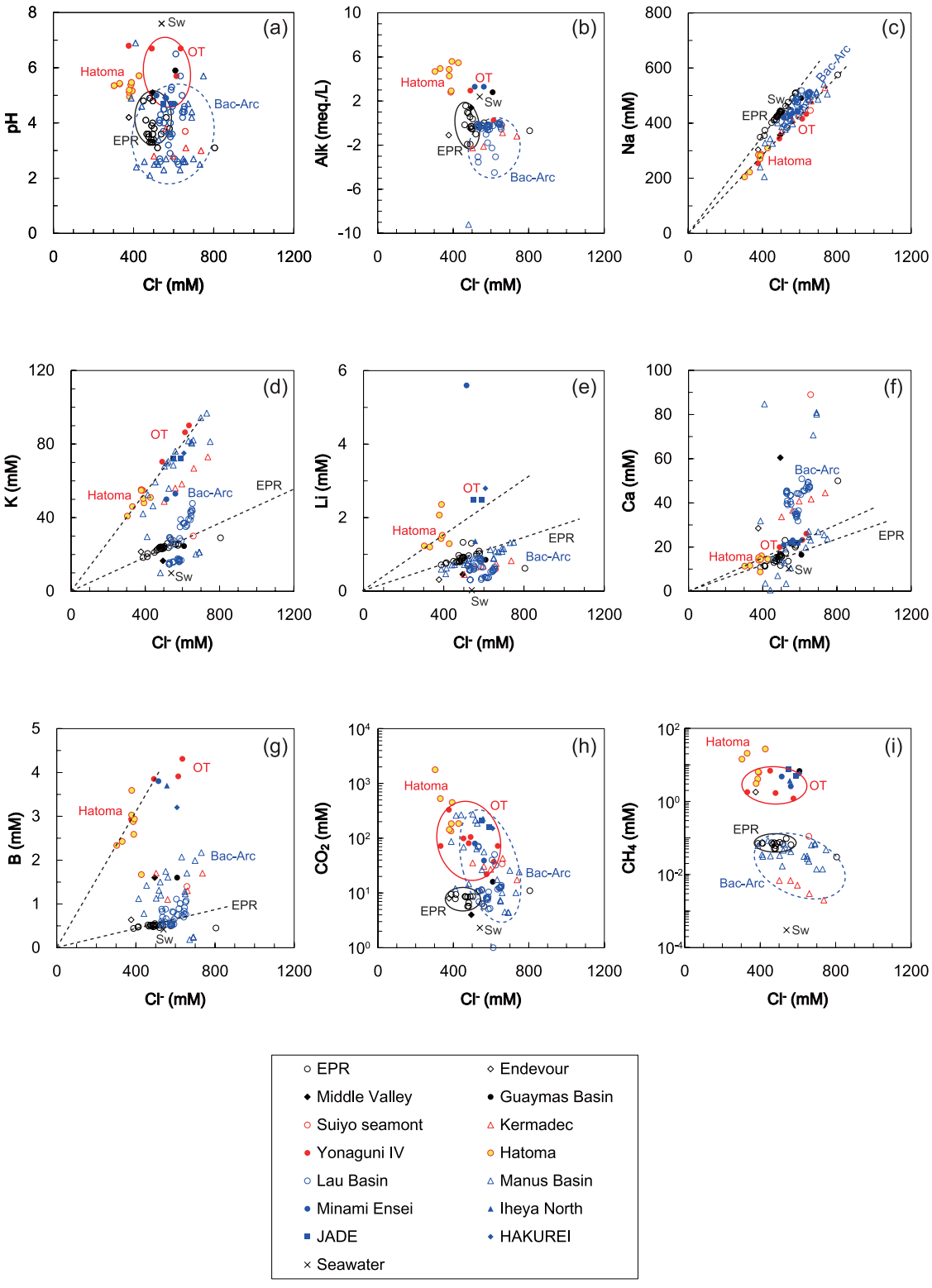

Fig. 5. Relationships between the pure hydrothermal fluid end-member concentration of each chemical component and the Cl^- hydrothermal fluid end-member concentration at each site of Hatoma Knoll: (a) pH, (b) alkalinity (Alk), (c) Na, (d) K, (e) Li, (f) Ca, (g) B, (h) CO_2, and (i) CH_4. Colors denote geological settings: black, MOR; red, arc; and blue, backarc. Open symbols denote sediment-starved systems, and filled symbols denote sediment-covered systems. In the Okinawa Trough, Yonaguni IV Knoll and Hatoma Knoll are located on the 200 km depth contour of the Wadati-Benioff zone, as shown in Fig. 1b, and belong to arc systems based on just only the geographical factor. In the same reason, the other hydrothermal systems belong to backarc systems.

lighting (Butterfield *et al*., 1990, 1994b; Hannington *et al*., 2001; Massoth *et al*., 1989; Stoffers *et al*., 2006). On the other hand, at Chura, the hydrothermal fluids only seeped from the seafloor. Moreover, at Iri, only one mound in a sand field was venting hydrothermal fluids, and macro-organisms, including *Bathymodiolus* and *Galatheidae*, had formed a colony with a diameter of several meters around the mound. Therefore, hydrothermal activity is high at Gusuku, but not as high at Chura and Iri. These activity levels can be related to proximity to subsurface heat source; Gusuku would be the closest to the heat source, located around the center of the crater. On the other hand, Chura would be far from the heat source, located on its western wall. Iri would be also far from the heat source, located in a sand field in the western part of the crater. Gusuku would be at the center of hydrothermal activity in Hatoma Knoll, whereas Chura and Iri are at some distance from the center.

pH and alkalinity The pH of the sample with the lowest Mg concentration at each site ranged from 5.0 to 5.7 (Table 2a). These values were measured at room temperature; thus, because the fluids had undergone degassing, these values are just a rough indication of the true values. They are significantly higher, however, than pH values of hydrothermal fluids in MORs, which range about 3–5 on average (Fig. 5a; Von Damm, 1995). Similar results have been reported for other sediment-covered hydrothermal systems, such as Okinawa Trough (4.7–6.8), Middle Valley (5.1), and Guaymas Basin (5.9), where they have been attributed to the decomposition of organic matter in the sediment (Von Damm *et al*., 1985a).

The end-members at all sites have positive alkalinity ranging from 3.0 to 8.6 meq./L (Table 2a). These values are higher than those of hydrothermal fluids in MORs (Fig. 5b), where hydrothermal fluid is neutralized by water-rock interactions at high temperature. The increased alkalinity have been reported for sediment-covered systems, including Okinawa Trough and Guaymas Basin (Fig. 5b), which is also responsible for organic decomposition in the sediment (Von Damm *et al*., 1985a). On the other hand, alkalinity of backarc and arc hydrothermal fluids are negative, which is completely different from the Hatoma alkalinity (Fig. 5b).

Anions Chloride (Cl^-) is a conservative element and in the Hatoma fluids it showed two end-members: one for the fluids venting at Gusuku and another for those venting at the other sites; Oritori, Agari, Iri, and Chura sites (Fig. 2a). The Cl^- concentration at the hydrothermal source was lower than the Cl^- concentration of seawater (550 mM), a result that suggests that the hydrothermal fluid boiled (i.e., underwent subcritical phase separation) (Bischoff and Pitzer, 1989). At Yonaguni IV, Cl-rich fluids and Cl-poor fluids compared with the Cl concentration of seawater vent from the hydrothermal systems (Suzuki *et al*., 2008), but only Cl-poor fluids vent from the Hatoma hydrothermal system. At Iheya North, where only vapor was detected on the seafloor, brine was detected below the seafloor during IODP Expedition 331 (Expedition 331 Scientists, 2010).

Sulfate ions (SO_4^{2-}) are generally precipitated as anhydrite ($CaSO_4$) during hydrothermal circulation above 130°C. Because anhydrite becomes less soluble with increasing temperature, hydrothermal fluids are generally free from SO_4^{2-} as well as Mg (Von Damm, 1995). However, the SO_4^{2-} concentrations deviate slightly from a 1-to-1 relationship with Mg, indicating a positive anomaly (Fig. 2b). It is possible that during the sampling procedure, some $CaSO_4$ became mixed with the samples and dissolved before the sample filtration. During sampling, we observed a white precipitate covering the seafloor, and newly built chimneys are composed mainly of anhydrite (i.e., $CaSO_4$; Okamoto *et al*., 2002). A covering of white sulfate mineral on the seafloor, observed after drilling, and sulfate precipitation is a distinctive feature of the Okinawa Trough hydrothermal fields (Kawagucci *et al*., 2013a).

Cations The alkali elements Na, K, and Li are conservative components, and they showed linear relationships relative to the Mg concentrations (Figs. 2d, 2e, and 2f). The Na concentrations showed a different linear relationship with Mg concentrations in fluid from Gusuku (red symbols) than in fluids from the other vents (Fig. 2d). Although both relationships were linear, most of the Gusuku samples were plotted below the line of the data from the other sites (Fig. 2d). These distributions can be attributed to phase separation, as described in section 5.3 for chloride. The Na end-member values at Gusuku ranged from 205 to 287 mM, whereas those at the other sites ranged from 283 to 310 mM (Table 2a). At all sites, the Na end-member concentrations are lower than the seawater concentration (460 mM). In Fig. 5c, the Na values are compared with those in MOR hydrothermal fluids. The Na/Cl ratios obtained from the Hatoma hydrothermal fluids are lower than the ratios in EPR hydrothermal fluids and the seawater ratio (Fig. 5c), and they are comparable to the ratios in Yonaguni IV fluid from the Okinawa Trough (Fig. 5c).

The K concentrations showed also two end-members, one for the Gusuku samples and another for the other samples (Fig. 2e). The K end-member values ranged from 40.8 to 54.7 mM at Gusuku and were lower than those at the other sites, which ranged from 50.4 to 55.2 mM (Table 2a). All K end-member values were higher than the seawater concentration (10 mM), and also higher than values in hydrothermal fluids in MOR systems (Fig. 5d). Such K enrichment has been detected in other hydrothermal systems related to arc-backarc systems, namely, other systems in the Okinawa Trough (Sakai *et al*., 1990b) and

the Manus Basin in the Bismarck Sea north of Papua New Guinea (Reeves *et al*., 2011), as well as at Hatoma Knoll (Nakano *et al*., 2001). The K enrichment is attributed to the interaction of the hydrothermal fluids with felsic host rocks of the hydrothermal systems (Nakano *et al*., 2001; Reeves *et al*., 2011; Sakai *et al*., 1990b). As shown in Fig. 5d, the K/Cl ratios in the Hatoma data are compatible with other Okinawa Trough data but not with MOR data.

The Li concentrations also showed two linear relationships relative to Mg concentrations (Fig. 2f); the Gusuku and Iri samples had relatively lower concentrations compared with samples from the other sites, although higher than the seawater concentration (28 μM). The Li was also probably derived from felsic host rocks of the hydrothermal system, but the enrichment was not as great as the K enrichment (Fig. 5e). Enrichment in Li, as well as in K, is a specific feature of Okinawa Trough hydrothermal fluids (Fig. 5e).

Ca and Sr were linearly related to the Mg concentration but with considerable scatter (Figs. 2g and 2h). These results suggest that when these samples were obtained, anhydrites became dissolved in the sampling tube or bottle, just as it may have occurred in the case of sulfate (see Subsection "Influences of sediments on Hatoma hydrothermal chemistry"). The end-member concentrations of Ca at all sites except C1 were higher than the seawater concentration of 10 mM (Table 2a). In contrast, the end-member concentrations of Sr at all sites were lower than the seawater concentration (87 μM) (Table 2a).

When the Ca end-members from Hatoma Knoll are compared with other hydrothermal end-members, their values correspond to those from the other hydrothermal fields in the Okinawa Trough, which are slightly higher than those from EPR (Fig. 5f). Other hydrothermal fields related to arc-backarc systems show Ca enrichment, but the hydrothermal fields in the Okinawa Trough do not show a very great enrichment more than 30 mM. The homogeneous Ca/Cl ratios in Okinawa Trough hydrothermal fluids are one of their distinctive features (Fig. 5f).

Ba concentrations showed a non-linear relationship with Mg concentrations (Fig. 2i), so we did not calculate an end-member value. The nonlinearity of the relationship of Ba to Mg can be explained by the low solubility of Ba at lower temperatures. Because most samples were not collected by a 'major' sampler (Table 1), as the hydrothermal fluid sample cooled, Ba would have precipitated out of solution and been removed during sample filtration. It is not due to seawater mixing, because Ba is not preserved even in Mg-free samples (Fig. 2i). It would be due to cooling after sampling in the bottle of the sampler and/or the tube between the inlet and the bottle of the sampler.

Mn concentrations were linearly related to Mg concentrations, and we identified two end-members, as with many of the other elements (Fig. 3a). The Mn end-member concentrations at Gusuku were 402–580 μM, and 473–659 μM at the other sites (Table 2a). Seawater contains very little Mn, so the end-member values are remarkably higher than the seawater concentration. Comparison of the end-member values at Hatoma with values for other hydrothermal fields in the world showed that they are equivalent to those of the EPR (data not shown).

Fe concentrations showed a non-linear relationship with Mg concentrations (Fig. 3b). As with Mn, the nonlinearity of the Fe to Mg relationships can be explained by the low solubility of Fe at lower temperatures. As the hydrothermal fluid sample cooled, Fe would have precipitated out of solution and been removed during sample filtration (Fig. 3b), like as Ba. We did not calculate Fe end-member values. In the Okinawa Trough, Fe does not show a linear relationship with the Mg concentration in hydrothermal fluids, and few end-member concentrations have been reported, except at Yonaguni IV Knoll. The Fe end-member concentration in the Yonaguni IV hydrothermal fluids is as low as 0.41 mM (Suzuki *et al*., 2008), lower than EPR values (~1 mM; Von Damm *et al*., 2002). The maximum concentration of Fe in this study is not as high as 0.01 mM (Fig. 3b), and it can be inferred, at least, that Fe concentrations in the Hatoma hydrothermal fluids are lower than EPR values.

The Al data are scarce and a general trend cannot be inferred, but the end-member concentrations calculated for each site ranged from 3.6 to 6.0 μM (Table 2a). These values are relatively low compared with reported concentrations in global hydrothermal fluids, though the data are poor.

Generally, the concentrations of these metals in sediment-covered hydrothermal systems are lower than those in sediment-starved systems because of the lower solubility of metals at lower temperature (Cruse and Seewald, 2001). Actually, the Okinawa Trough is a sediment-hosted arc-backarc system, and all of its hydrothermal systems showed lower metal concentrations than those of MORs (Table 2a). It implies the Okinawa Trough hydrothermal fluids may have higher temperature than those observed at the seafloor, and the covering sediments could facilitate subsurface cooling and re-equilibration at relatively low temperature before venting at the seafloor to decrease metal concentrations. The metal-poor character of the Okinawa Trough hydrothermal fluids compared with sediment-starved MOR hydrothermal fluids is another distinguishing feature of Okinawa Trough hydrothermal systems.

Si, I, NH_4^+, and B Si is a neutral species, and its relationship with Mg concentrations is similar to those of the alkali elements (Fig. 3d). All of the Si end-member values were higher than the seawater concentration (Table 2a).

Those at Gusuku ranged from 6.4–11.3 mM, whereas those at other sites were 8.3–13.0 mM, which shows that Si was enriched at the other sites more than at Gusuku. This result is consistent with the distribution of the other components. Si is expected to equilibrate with quartz, which is one of the main components of many rocks, according to the equilibrium temperature and pressure, that is, water depth (Von Damm *et al*., 1991). Si concentration of a hydrothermal fluid has been used for evaluation of the equilibrium temperature and pressure between the hydrothermal fluid and quartz (Von Damm *et al*., 1991).

I, NH_4^+, and B concentrations were linearly related to Mg concentrations (Figs. 2c, 3e, and 3f). The concentrations of each showed two main end-members, one for the Gusuku site and the other for other sites (Figs. 2c, 3e, and 3f). The NH_4^+ distribution in particular differed between Gusuku and the other sites, with Gusuku samples having higher concentrations. This finding removes doubts that the Gusuku samples might have been contaminated by the ultrapure water that was used to fill the gas-tight bottles of the WHATS and C-WHATS samplers before each dive. The distribution of NH_4^+ suggests NH_4^+ would behave as one of components concentrated in vapor when a hydrothermal fluid boils; for example as NH_3 (Butterfield *et al*., 2003). The end-member concentrations of I, NH_4^+, and B were calculated (Table 2a). All three were more abundant in the hydrothermal fluid than they are in seawater, and their concentrations are extremely high compared with those in sediment-starved hydrothermal systems (Fig. 5g). I, NH_4^+, and B can originate from the decomposition of organic matter (Lilley *et al*., 1993; You *et al*., 1994), and their enrichment is a distinctive feature of hydrothermal chemistry in the Okinawa Trough, where the seafloor is covered by a large amount of sediments (Ishibashi *et al*., 1995; Kawagucci *et al*., 2011, 2013b; Suzuki *et al*., 2008).

Gaseous components The CO_2, H_2S, CH_4, H_2, C_2H_6, C_3H_8, He, and ^3He concentrations showed non-linear relationships with Mg concentrations (Figs. 4a–g). Because hydrothermal fluids undergo phase separation beneath the seafloor, the end-member concentrations of these gaseous components could not be determined using a linear relation to the Mg concentrations, so the maximum concentrations among the samples from each vent are listed in Table 2b.

These values of CO_2 ranged from 97 to 1770 mM (Fig. 4a), all of which are definitely higher than the concentrations from EPR (Fig. 5h), of which the upper limit is in excess of CO_2 solubility at the seafloor (Duan and Sun, 2003). This result is similar to results reported for other hydrothermal systems related to arc-backarc systems or sediment-covered systems (Fig. 5h). The high concentrations are attributable to influences from subducting materials or covering sediments (Ishibashi *et al*., 1995; Sakai *et al*., 1990b). The hydrothermal systems of the Okinawa Trough, where the world's first CO_2 hydrates were discovered at Izena Hole (Sakai *et al*., 1990a) and a "lake" of liquid CO_2 was pointed out beneath the surface at Yonaguni IV Knoll (Inagaki *et al*., 2006), are representative for the CO_2 enrichments in hydrothermal fluids. Hydrothermal fluids in the Okinawa Trough contain a large amount of CO_2 relative to other hydrothermal systems; Izena Hole (Ishibashi *et al*., 1995), Iheya North Knoll (Kawagucci *et al*., 2011), and Minami-Ensei Knoll (Kawagucci *et al*., 2013b). Thus, a high CO_2 concentration is another distinctive feature of Okinawa Trough hydrothermal chemistry.

The highest concentrations of H_2S among the samples from each vent range from 13.5 to 40.9 mM (Table 2b). As mentioned above, in our sampling for H_2S analysis, the samples are inevitably suffered to degassing, and the H_2S data are the minimum value for the samples. Even though the data are the minimum value, they are apparently higher than the concentration in seawater, which contains hardly any H_2S. Moreover, when compared with concentrations in MORs (EPR: 3.3–8.7 mM), the Hatoma values are relatively higher. The high concentrations are comparable to those of the Manus hydrothermal fluids; 1.4–20.8 mM (Reeves *et al*., 2011). In the H_2S concentration, the other Okinawa Trough hydrothermal fluids are not so high; 4.5 mM for Iheya North (Kawagucci *et al*., 2011), 5.6 mM for JADE (Ishibashi *et al*., 2014), and 5.3 mM for HAKUREI (Ishibashi *et al*., 2014). As mentioned-above based on the metal concentrations (see Subsection "End-members of the Hatoma hydrothermal fluids"), H_2S generally precipitate as sulfide in subsurface sediments in sedimented hydrothermal systems (Cruse and Seewald, 2001), and the Okinawa Trough hydrothermal fluids are no exception based on the observed metal concentrations (see Subsection "End-members of the Hatoma hydrothermal fluids"). Even though sulfide precipitation occurred, hydrogen sulfide concentrations in the Hatoma hydrothermal fluids are very high up to 40.9 mM, which would be due to phase separation and the Hatoma hydrothermal fluids are very gas-rich fluids including H_2S, CO_2, and the other gases, especially C2 vent in Gusuku site (Table 1b). This fact support also the view that Gusuku site is the most active site.

The CH_4 maximum concentrations ranged from 2.9 to 20.8 mM (Table 2b), which are obviously higher than the concentration in seawater, which has a CH_4 concentration of several nanomolars. When the CH_4 maximum concentrations at Hatoma are compared with those of other hydrothermal fluids in the world, they occupy the high end of the concentration range (Fig. 5i). Other Okinawa Trough hydrothermal fluids show CH_4 concentrations similar to those of the Hatoma fluids (Fig. 5i). The C_2H_6 maximum concentrations ranged between 11.0 and 40.0

μM (Table 2b). C_3H_8 was not detected in most samples, and the C_3H_8 maximum concentrations ranged from 33 nM to 3.8 μM (Table 1b).

The H_2 maximum concentrations ranged between 41 and 1228 μM (Table 2b); these values are higher than the concentration in seawater and comparable to EPR and Yonaguni IV values. They are also higher than concentrations in arc hydrothermal systems, and lower than those in ultramafic-rock-hosted hydrothermal systems. H_2 originates from fluid-basalt interaction (Seyfried Jr. and Ding, 1995; Seyfried Jr. *et al*., 1991), organic matter oxidation in sediment at high temperature condition (Cruse and Seewald, 2006), microbial fermentation in sediment column at relatively lower condition (Dolfing, 1988) or from serpentinization of olivine in ultramafic rocks (Charlou *et al*., 2002). Ultramafic rocks and serpentine, however, have never been observed in the Okinawa Trough, though felsic rocks and sediments have often been reported (see references in Glasby and Notsu (2003)). In the Okinawa Trough, H_2 concentrations in the hydrothermal fluids show a significant variation; 1–62 μM for Minami-Ensei (Kawagucci *et al*., 2013b), 230 μM for Iheya North (Kawagucci *et al*., 2011), 50–60 μM for JADE (Ishibashi *et al*., 2014), 1.35 mM for HAKUREI (Ishibashi *et al*., 2014), 0.8–3.8 mM for Yonaguni IV (Konno *et al*., 2006). The Hatoma data, 41 μM–1.23 mM, fall into the Okinawa Trough range; 1 μM–3.8 mM. Compared to the EPR hydrothermal fluids containing H_2 from 30 μM to 3 mM (Von Damm *et al*., 2002), the Okinawa Trough hydrothermal fluids do not contain so much H_2. These values are higher than those of the Manus Basin (2.4–300 μM; Reeves *et al*., 2011) and the Kermadec arc (8.7–72 μM; de Ronde *et al*., 2011; Takai *et al*., 2009).

He was scarcely detected (Table 1b), and its concentrations were not linearly related to Mg concentrations (Fig. 4f). In Table 2b, we list the highest value, 1.2 μM, which was detected at 189-1. Reported He concentrations in global hydrothermal systems range from 0.3 to 2.78 μM. Those detected in the Hatoma hydrothermal fluids fall within this reported range. Concentrations of ^{3}He were calculated from He concentrations and ^{3}He/^{4}He ratios. The relationship between ^{3}He and Mg was similar to that of He with Mg (Fig. 4g). The highest measured value around 10 pM (Fig. 4g), falls within the range of values from other hydrothermal systems (3.3–31.5 pM).

Isotopes End-member isotope ratios of CH_4 are estimated from the intercept of the y-axis when the isotope ratio is plotted against the reciprocal of its concentration (Keeling, 1961). Estimates of this type are based on the assumption that the background concentration is negligible relative to the end-member concentration. In the case of methane, the background CH_4 concentration in seawater is several nanomolars, whereas that in hydrothermal fluid is several tens of millimolars, a seven order of magnitude difference. The $\delta^{13}C(CH_4)$ values showed a nonlinear relationship with $1/CH_4$. At Gusuku, $\delta^{13}C(CH_4)$ in CH_4-rich samples were between –53.1‰ and –49.1‰ (all values are relative to VPDB), and at the other sites they were –54.5‰ and –49.5‰ (Table 2b). Although the Gusuku samples showed more scattering than the other samples, the range of values was not very different; in both cases the average was around –52‰. $\delta^{13}C(CH_4)$ values in fluids from unsedimented MOR hydrothermal systems measured to date range from –20.8‰ to –8.0‰ (McCollom and Seewald, 2007), whereas in sedimented hydrothermal fluids at Juan de Fuca Ridge (JFR) they range from –56‰ to –43‰ (McCollom, 2008; Proskurowski *et al*., 2006), and they range from –55‰ to –25‰ in the Okinawa Trough (Ishibashi *et al*., 1995; Kawagucci *et al*., 2011, 2013b; Konno *et al*., 2006). The lowest $\delta^{13}C(CH_4)$ reported value among Okinawa Trough hydrothermal fluids is from Iheya North Knoll, –55‰ (Kawagucci *et al*., 2011). The Hatoma $\delta^{13}C(CH_4)$ values are therefore similar to the Iheya North value.

End-member isotope ratios of CO_2 are estimated from mass balance equation below:

$$[CO_2]_{obs} \times \delta^{13}C(CO_2)_{obs} = (1 - t) \times [CO_2]^* \times \delta^{13}C(CO_2)^* + t \times [CO_2]_{sw} \times \delta^{13}C(CO_2)_{sw} \quad (2)$$

where $[CO_2]$ is the concentration of CO_2, $\delta^{13}C(CO_2)$ is the carbon isotopic composition of CO_2, t is the mixing ratio of hydrothermal fluid in the sample (calculated from the measured Mg concentration), the subscripts obs and SW refer to the sample and seawater components, respectively, and the super script * refers to the end-member component. The end-member $\delta^{13}C(CO_2)$ values determined in this manner ranged from –16.2‰ to –3.4‰ (Table 2b), all of which are lower than the seawater ratio (0‰), but they have a wide range more than that of other unsedimented MOR hydrothermal fluids (–13.0‰ to –3.2‰) (Charlou *et al*., 1996, 2002; McCollom and Seewald, 2007).

The ^{3}He/^{4}He ratios (R/R_A) ranged from 0.41 to 7.23, where R is the sample ratio and R_A is the ratio in air (Table 1b). The ^{4}He/^{20}Ne ratios ranged between 0.17 and 232. ^{20}Ne is extraordinarily enriched in the air and seawater relative to in the mantle and crust, so it is used to calculate a corrected helium isotope ratio for mixing with seawater, under the assumption that all ^{20}Ne is ultimately derived from the air (Craig *et al*., 1978):

$$R_C/R_A = (R/R_A \times N_{obs}/N_{ASW} - 1)/(N_{obs}/N_{ASW} - 1), \quad (3)$$

where R_C/R_A represents the corrected helium isotope ratio, N_{obs} the observed ^{4}He/^{20}Ne value, and N_{ASW} the ^{4}He/^{20}Ne ratio in seawater equilibrated with air (0.25) (Sano

et al., 2006). We calculated the average (±standard deviation) of the corrected helium isotope ratio at each site (Table 2b). Here, we excluded samples with $^4He/^{20}Ne$ ratios of less than 1 from further analysis because the corrected values showed large errors. The corrected helium isotope ratios in the Hatoma hydrothermal fluids were 5.9–7.2 (Table 2b). The helium isotope ratios at Chura were slightly lower than those at the other sites. The Hatoma values are lower than those in MOR hydrothermal fluids (around 8.09 ± 0.49) (Sano and Fischer, 2013), and values in sediment-starved backarc hydrothermal fluids are between 7.4–12.0 (Fourre *et al*., 2006), which overlap 7.72–7.83 for the Lau Basin (Takai *et al*., 2008b), 8.04–10.0 for the North Fiji Basin (Ishibashi *et al*., 1994), 8.5 for Alice Springs (Ishibashi *et al*., 2015), and 8.09–8.37 for the southernmost Mariana Trough near 13°N (Toki *et al*., 2015). Although the values in sediment-starved arc hydrothermal fluids are between 6.59–8.35 (Lupton *et al*., 2008), which overlaps the values in the other sediment-starved arc hydrothermal fluids; 8.1 for Suiyo Seamount (Tsunogai *et al*., 1994), 8.01 for Forecast field (Ishibashi *et al*., 2015), and 6.9–7.2 for Brother Seamount (de Ronde *et al*., 2011), the Hatoma values are lower than the lowest value among those in sediment-starved arc hydrothermal fluids. The Hatoma values correspond to reported values from other hydrothermal fluids in the Okinawa Trough: 7.0 from Minami-Ensei (Kawagucci *et al*., 2013b), 7.1 from Iheya North (Kawagucci *et al*., 2011), 5.8 from JADE (Ishibashi *et al*., 1995), and 4.7–6.5 from HAKUREI (Ishibashi *et al*., 2014). Thus, although the Hatoma values vary widely (5.9–7.2), they fall within reported ranges for Okinawa Trough hydrothermal fields.

The oxygen isotopic composition ($\delta^{18}O$) of H_2O in the hydrothermal fluid showed two end-members (Fig. 4h); the values calculated for Gusuku were +1.1‰ to +2.2‰, which are relatively lower than those calculated for the other sites, +1.9‰ to +2.1‰ (Table 2b). Both sets of end-member values are higher than the seawater value of around 0‰. The hydrogen isotopic ratios of H_2O in the hydrothermal fluid (δD) were scattered (Fig. 4i); the range of the calculated end-member values at Gusuku (–6.7‰ to –2.7‰) was particularly broad (Fig. 4i), compared with –4.8‰ to –2.4‰ at the other sites (Table 2b). The values in both cases are lower than the seawater ratio of around 0‰. The isotope data in the Hatoma fluids (i.e., positive $\delta^{18}O$ and negative δD values) are different from those in the MOR fluids having both positive $\delta^{18}O$ and δD (Shanks, 2001; Shanks *et al*., 1995), and qualitatively the same as reported values from backarc systems related to silicic arc magma (Mottl *et al*., 2011; Reeves *et al*., 2011).

Phase separation beneath the seafloor

The end-member concentration of each component is plotted against the end-member concentration of Cl^- at each site in Fig. 5. Even though their absolute values show a variation for each site (Table 2), the data points lie on straight lines passing through the origin, and in general the ratio of each component to that of Cl^- is specific to Hatoma Knoll. There are several exceptions, namely, Si, CO_2, CH_4, and H_2, and the latter three are volatile components. These results suggest that the hydrothermal fluids were derived from a single hydrothermal source, and that the fluids boiled beneath the seafloor, causing segregation of vapor and brine (Berndt and Seyfried Jr., 1993). Thus, although it might seem that the hydrothermal system includes multiple hydrothermal sources, the hydrothermal fluids are in fact derived from a single source that has undergone phase separation (Butterfield *et al*., 1994b; Foustoukos and Seyfried Jr., 2007; Foustoukos and Seyfried, 2007). As a result, dissolved ions have become concentrated in the liquid phase and volatile components have become concentrated in the vapor phase. In fact, the lower the end-member Cl^- concentrations were, the higher the concentrations of volatile components tended to be (Figs. 5h and 5i), supporting the inference that phase separation occurred beneath the seafloor prior to venting from the seafloor.

The end-member Si concentration of a hydrothermal fluid can be used to estimate the temperature and pressure conditions at which the hydrothermal fluid equilibrated with quartz (Von Damm *et al*., 1991). We therefore plotted end-member Si concentrations against maximum observed hydrothermal fluid temperatures (Fig. 6). By assuming a maximum temperature of 325°C and a water depth at the seafloor of 1500 m (Table 1a), we calculated the equilibrated concentration of Si with quartz to be about 13.5 mM in the hydrothermal fluid (a star in Fig. 6). The detected concentrations of Si in the hydrothermal fluids from Hatoma Knoll, however, do not reach this value. Low-Cl^- fluids have usually low-Si contents for effects of phase separation (Von Damm *et al*., 1991). It suggests the fluids do not reach re-equilibrium conditions for Si with quartz at the seafloor. Instead, the hydrothermal fluids must boil just before venting from the seafloor, preventing the Si concentrations from achieving equilibrium with quartz in the hydrothermal fluids.

As mentioned in Subsection "End-members of the Hatoma hydrothermal fluids", especially the Gusuku fluids were venting as a flame-like appearance, caused by a small jet of H_2O vapor (Butterfield *et al*., 1990, 1994b; Hannington *et al*., 2001; Massoth *et al*., 1989; Stoffers *et al*., 2006). This is the visual evidence of phase separation at the seafloor of ~1474 m depth. Theoretically, when the 2-phase boundary for seawater at this depth is ~340°C (Bischoff and Rosenbauer, 1985), but the temperature is only 320–325°C (Table 1a). Nevertheless, the widespread compositional variability shown in very low-Mg samples

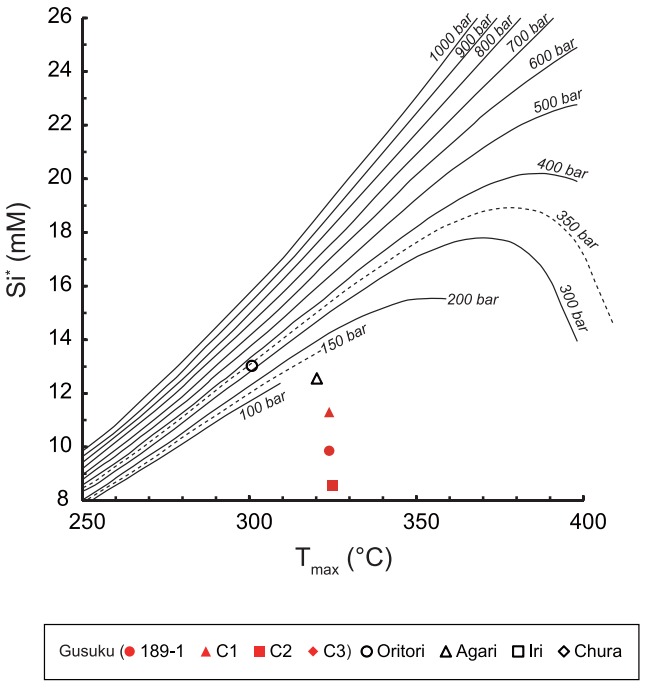

Fig. 6. End-member Si concentrations and maximum temperatures observed at each site in the Hatoma hydrothermal field. In addition, quartz saturation curves from (Von Damm et al., 1991) are shown for pressures of 100–1000 bars as a function of temperature.

for the Gusuku samples, both for gases and anions/cations (Figs. 2–4), suggests each individual sample of vent fluid can contain differing vapor versus brine ratios and gases. This is simply due to *in-situ* phase separation and partial/incomplete segregation. Thus, many evidences show phase separation is occurring at the seafloor, but the measured temperatures are too low for boiling at the seafloor. This discrepancy between temperatures and compositions/observations could be explained by extraordinarily high CO_2 concentrations, likely near or above solubility at seafloor conditions. Generally, when some gases, including CO_2, input into hydrothermal fluids, phase separation can occur at higher pressure compared to the occurrence without a gas input (Takenouchi and Kennedy, 1964). Actually, we observed gas bubbles at C2 vent at Gusuku site as shown in Table 1a, and in this case, phase separation means CO_2 gas bubble formation rather than water-steam separation. Thus, below the boiling point of seawater, CO_2 bubble forms to perform a 'flashing' phenomenon and fake chemical compositions similar to occurrence of phase separation.

Comparison of the chemical components among the sites shows that the Cl^- concentration was lowest at Gusuku, in particular at the C2 vent. Thus, we infer that active phase separation occurs in the subsurface in the C2 vent at Gusuku. The maximum observed temperature of the hydrothermal fluid was also recorded at the C2 vent (Table 1a). Together, these results suggest that the highest level of hydrothermal activity occurs at the Gusuku C2 vent. The Gusuku vent site is nearest to the heat source, followed by Agari and Oritori; Chura, on the western wall of the crater, is relatively far from the heat source in Hatoma Knoll. The distribution of hydrothermal vents in the Hatoma crater can be seen in other caldera/crater systems (de Ronde *et al*., 2011), where hydrothermal vents distribute at the center of caldera and the rims of caldera, because usually faults around the rims of caldera can provide very good conduits for fluid flow. At Brothers volcano of the Kermadec arc, two distinct vent fields, the Cone and NW Caldera sites, exhibit entirely different hydrothermal fluids (de Ronde *et al*., 2011). At the Cone site, corresponding to the highest peak in the Brothers, gas-rich hydrothermal fluids diffuse at low temperatures (≤122°C) with acidic and metal-poor. On the other hand, the NW Caldera site is located at the rim of the Brothers Caldera, and focused, hot, moderate acidic, metal-rich, and gas-poor fluids are venting. In the case of the Brothers, presumably faults at the rim of the caldera would allow focusing of fluids (de Ronde *et al*., 2011). At the Hatoma system, the Chura and Iri sites are located at the rims of the crater, but they are venting only low-temperature fluids, up to 75°C and 226°C, respectively (Table 2). In this study, below the rim sites, possible faults could be not so large conduits to flow focused fluids at high temperature. Thus, the most vapor-rich fluids are venting from the C2 vent at Gusuku around the center of the crater. The characteristics of the hydrothermal fluid distribution at Hatoma Knoll are unusual among hydrothermal systems in the Okinawa Trough. In general, vapor-rich hydrothermal fluids are found farthest from the heat source because of the high mobility of vapor (Kawagucci *et al*., 2011; Suzuki *et al*., 2008). However, the hydrothermal fluids at Gusuku are both the hottest and the most vapor rich in the Hatoma hydrothermal field. A possible explanation is that bubbling occurs just beneath the seafloor at Gusuku, so that the vapor phase does not have time to move very far. On the other hand, the brine phase, which is where salts not incorporated in the vapor phase should be, may be just missing, or it may remain below the seafloor (Expedition 331 Scientists, 2010).

Thus, phase separation occurs in the Hatoma hydrothermal system, and the system would have a single hydrothermal reservoir. Additionally, contrary to the other hydrothermal systems in the Okinawa Trough, the vapor phase does not move so far, because boiling could occur just beneath the seafloor. That could make Si concentrations in the fluids not equilibrated with quartz at *in-situ* temperature and pressure conditions. Moreover, as another characteristic, brine was not detected yet.

Fluid-rock interaction at the Hatoma hydrothermal system

Hydrothermal chemistry is controlled by temperature, pressure, and the chemical compositions of host rocks (Von Damm, 1995). Hydrothermal systems at Hatoma Knoll in the Okinawa Trough show compositions poor in Na, and rich in Ca, K, and Li relative to EPR (Fig. 5), suggesting that the host rocks of the Hatoma hydrothermal systems are different from those of EPR (i.e., MORB). In fact, basalts and rhyolites are distributed at Hatoma Knoll in the Okinawa Trough, and the compositions of the basalts differ from that of MORB (Shinjo *et al.*, 1999). These host rocks contain an abundance of incompatible elements, dissolved elements in a liquid phase in equilibrium between solid and liquid phases rather than incorporated in a solid phase, such as K and Li, and they are characteristically observed in magma related to arc-backarc systems. The content of K in the volcanic rocks in the Okinawa Trough is around 10 times higher than that of MORB (Shinjo and Kato, 2000; Shinjo *et al.*, 1999). Moreover, the presence of terrigenous sediments from the Eurasian continent or Taiwan is a noteworthy characteristic of the Okinawa Trough (Dou *et al.*, 2010a). These sediments are composed mainly of illite (Diekmann *et al.*, 2008). A formula of illite is $K_{0.65}Al_{2.0}[Al_{0.65}Si_{3.35}O_{10}](OH)_2$, which corresponds to K of 7%. On the other hand, chemical composition of MORB is 0.2% as K_2O, corresponding to 0.08% as K (Melson *et al.*, 2013). Thus, illite is generally rich in K relative to MORB. The Hatoma hydrothermal systems in the Okinawa Trough are hosted by different rocks and/or sediments than MOR systems, and it would be the reason why the Hatoma hydrothermal fluids show a different chemistry from that of MOR hydrothermal fluids.

The positive $\delta^{18}O$ and negative δD values of the pure hydrothermal fluids for all Hatoma Knoll sites are plotted in Fig. 7, in which the isotopic ranges of possible fluid sources and the direction of isotopic shifts due to phase separation and fluid reactions with basalt and sediments are also illustrated. Although hydrothermal fluids are originated from seawater, as shown in Fig. 7, the isotope ratios of the Hatoma hydrothermal fluids deviate from those of seawater (in which both $\delta^{18}O$ and δD are 0‰), suggesting that the hydrothermal fluids have mixed with other sources than seawater or that the isotope values have shifted as a result of reactions between originated seawater and ambient solid phases during fluid circulation. Because hydrothermal systems are associated with a heat source such as magma, which is derived from the upper mantle, primordial water in the mantle is another possible fluid source (Ohmoto, 1986; Taylor, 1979). However, the observed isotopic signatures do not lie on the trend line predicted by simple mixing between mantle-derived water and seawater (Fig. 7). Nor can a shift due to reactions

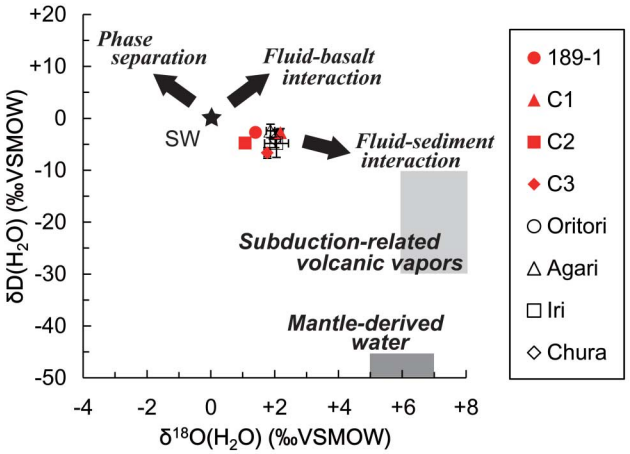

Fig. 7. End-member $\delta^{18}O$ and δD values from the Hatoma vent field, with postulated compositions of mantle-derived water (Ohmoto, 1986; Taylor, 1979) and subduction-related volcanic vapors (Giggenbach, 1992; Hedenquist and Lowenstern, 1994). Arrows indicate shifts due to reactions of hydrothermal fluids with sediment or basalt (Shanks et al., 1995; Von Damm et al., 2005).

between the fluid and basalt account for the signatures (Shanks *et al.*, 1995). Phase separation results in negative $\delta^{18}O$ and positive δD values in the vapor phase (Foustoukos and Seyfried, 2007). As described above, the chemical features of the Hatoma hydrothermal fluids indicate the occurrence of phase separation; in particular, Cl^- concentrations at Gusuku are lower than at the other sites, suggesting that phase separation has influenced the chemistry at Gusuku. The $\delta^{18}O$ and δD values at Gusuku are slightly more negative and more positive, respectively, than at the other sites (Fig. 7), suggesting an effect of phase separation. However, as regards the overall trend, the shift of the end-members to more negative $\delta^{18}O$ and more positive δD values cannot be explained by the effect of phase separation. Therefore, phase separation does not mainly control the isotopic compositions of the Hatoma hydrothermal fluids.

A leading candidate explanation for the observed features at Hatoma, subducted water, has positive $\delta^{18}O$ and negative δD values, because of degassing from felsic magma (Giggenbach, 1992; Hedenquist and Lowenstern, 1994). In fact, fluids with positive $\delta^{18}O$ and negative δD values have been observed in a shallow hydrothermal system in Kagoshima Bay, along the Ryukyu Arc (Ishibashi *et al.*, 2008), and in other hydrothermal systems in arc-backarc systems (Mottl *et al.*, 2011; Reeves *et al.*, 2011), and these values have been attributed to the influence of subducted water. As shown in Fig. 7, the Hatoma isotopic compositions seem to lie along a trend line for simple mixing between seawater and subducted

water, suggesting that the hydrothermal source was influenced by felsic magmatic water. This inference is consistent with the geological setting of Hatoma Knoll in an arc-backarc system (Sibuet *et al*., 1987). Furthermore, another leading candidate explanation for the positive $\delta^{18}O$ and negative δD values is that they are produced by extensive reactions between hydrothermal fluids and sediments covering the hydrothermal systems (Shanks *et al*., 1995). The presence of overlying sediments is an important characteristic of hydrothermal systems in the Okinawa Trough. Thus, the isotopic signatures can be explained either by the mixing of seawater with subduction-related volcanic vapors or by fluid-sediment interactions, or both (Fig. 7). Although we cannot isolate the cause of these isotopic signatures, it is certain that the water isotopes did not derive from reactions with only basalts. It is clear that the water isotopes of the Okinawa Trough hydrothermal systems differ from those of MOR systems, in which reactions occur only with MORB (Shanks *et al*., 1995).

Influences of sediments on Hatoma hydrothermal chemistry

We compared He isotope ratios in MOR hydrothermal systems (Fig. 8, black symbols) with those in backarc systems (blue symbols) and in arc systems (red symbols), as well as with the ratios in sediment-covered systems (filled symbols). In MOR hydrothermal systems, He isotope values are around 8, those in backarc systems are mainly higher than 8, and those in arc systems are around 8 (Fig. 8). In all three types of hydrothermal system, however, the values are lower when the systems are sediment covered than when they are sediment starved. Moreover, the Okinawa Trough hydrothermal systems have the lowest values among world hydrothermal systems (Fig. 8). The He isotope ratios in the arc hydrothermal fluids do not show such low values, indicating that subducting materials including oceanic crust and sediments do not lower the ratios in the hydrothermal fluids. The thing lowering the ratios would be covering sediments on the hydrothermal systems. In the Okinawa Trough, the covering sediments are derived from Eurasian continental crust or Taiwan (Dou *et al*., 2010a), and this old continental crust is rich in U and Th, which means that much ^4He is supplied by radioactive decay. This ^4He is then supplied to the hydrothermal fluids, leading to their having lower He isotope ratios. As a way of the supply, the hydrothermal fluids react with the sediments, of course. As another way, pore water in the sediments is enriched in ^4He, and when the pore water is recharged in the hydrothermal system, it would lead the hydrothermal fluids to increase of ^4He. In either way, it indicates the covering sediments have some impacts on the hydrothermal chemistry. Such an interpretation is supported by the enrichments of I, NH_4^+, and B, the components derived from organic matter (e.g., Fig. 5g).

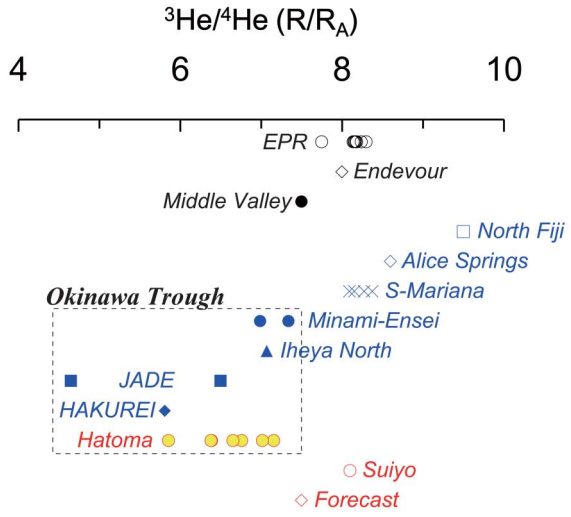

Fig. 8. Comparison of He isotopic compositions among hydrothermal fluids in various parts of the world, where data for mid-ocean ridges are colored by black, those for arc systems by red, and for backarc systems by blue. Additionally, the data for sediment-hosted hydrothermal systems are presented by solid symbols, while those for sediment-starved hydrothermal systems by open symbols.

Carbon isotope ratios of CO_2 in the hydrothermal fluids at Hatoma Knoll differ from site to site, ranging from –16.2‰ at Iri to –3.4‰ at Gusuku (Table 2). Carbon dioxide in hydrothermal fluids can originate from either organic carbon or inorganic carbon. The range of carbon isotope ratios differs depending on the origin of the CO_2, as shown in Fig. 9 (Jenden *et al*., 1988). The carbon isotope ratios associated with CO_2 from organic matter depend on the degradation process. In general, degradation of organic matter results in CO_2 $\delta^{13}C$ values of –30‰ to –20‰ (Jenden *et al*., 1988). In a semi-closed surface sediment system, however, methane oxidation coupled with sulfate reduction occurs, resulting in CO_2 $\delta^{13}C$ values lower than –30‰. In contrast, in oil fields, carbon dioxide produced by secondary methanogenesis has extraordinary ^{13}C-rich isotope ratios, as high as +20‰. CO_2 from inorganic carbon sources has a $\delta^{13}C$ value between –10‰ and 0‰. Such values have been detected in MOR hydrothermal fluids along with ^3He-rich He isotope ratios. CO_2 in seawater has a $\delta^{13}C$ value of around 0‰. Hydrothermal fluids are originated from seawater, the seawater permeates rocks and sediments, and reacts with those solids of seafloor. Or volcanic gases input into the fluids, and the chemistry changes from that of the original seawater. As the first step, CO_2 in the seawater has $\delta^{13}C(CO_2)$ = 0‰, and the seawater encounters carbonates and organic

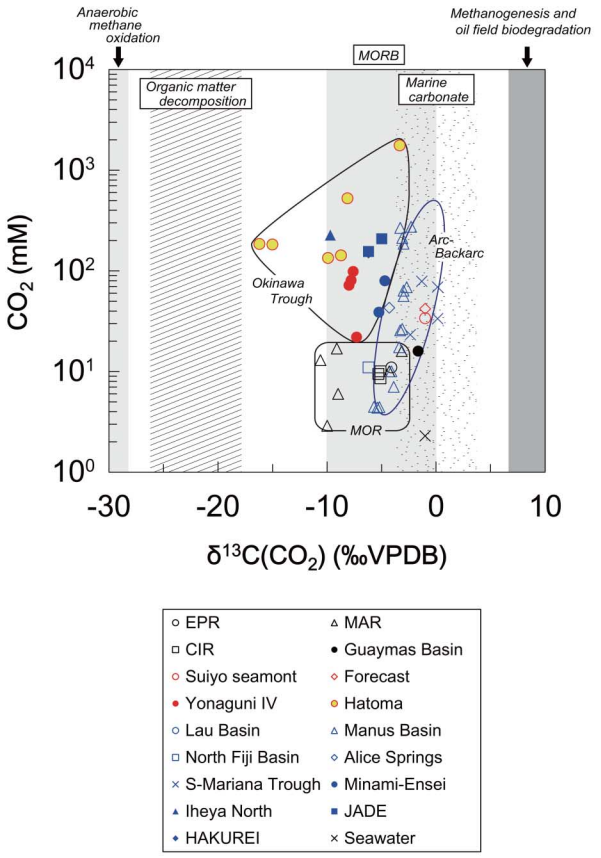

Fig. 9. Relationship between $\delta^{13}C(CO_2)$ and CO_2 in dissolved gases in hydrothermal fluids from all of the sites of the Hatoma hydrothermal system and in natural gases. The shaded areas are defined based on values of $\delta^{13}C(CO_2)$ reported by Jenden et al. (1988). Symbols as in Fig. 8. The data from Von Damm et al. (2002) for EPR, Charlou et al. (2002) for MAR, Kumagai et al. (2008) for CIR, Welhan and Lupton (1987) for Guaymas Basin, Tsunogai et al. (1994) for Suiyo seamount, Gamo (1995) for Forecast, Konno et al. (2006) for Yonaguni IV Knoll, Mottl et al. (2011) for Lau Basin, Reeves et al. (2011) for Manus Basin, Ishibashi et al. (1994) for North Fiji Basin, Gamo (1995) for Alice Springs, Toki et al. (2015) for the Southern Mariana Trough, Kawagucci et al. (2013b) for Minami-Ensei Knoll, Kawagucci et al. (2011) for Iheya North Knoll, Ishibashi et al. (2014) for JADE and HAKUREI sites in Izena Caldron.

carbon beneath the seafloor. Carbonates produced by plankton in seawater have $\delta^{13}C$ values of around 0‰, and these carbonates are found in seafloor sediments. Carbonate contents in seafloor sediments, inorganic carbon ratios, are area dependent; in the MOT, they are about 16% and in the SOT, they are about 7% (Chang *et al.*, 2005). Organic carbon ratios in both these areas are about 0.6% (Chang *et al.*, 2005). For comparison, a sediment trap deployed in an area seaward of the Ryukyu Trench trapped about half as much organic carbon and a quarter as much inorganic carbon as are found in MOT area (Honda *et al.*, 1997). The carbon isotope ratios of the covering sediments in the Okinawa Trough and of subducting materials in the Ryukyu Trench can be estimated from the proportions of organic and inorganic carbon in the materials in each area. The estimated carbon isotope ratio of the covering sediments is about –1‰, and that of the subducting materials to be about –2‰. Volcanic gases are a mixture of CO_2 of MOR systems with that in the subducting materials. For example, the carbon isotope ratio of subducting materials in Izu-Ogasawara Trench was estimated to be –1.2‰ by assuming that organic carbon composed <1% and inorganic carbon 7% of the subducting sediments (Tsunogai *et al.*, 1994). This fact can be found, as shown in Fig. 9, that $\delta^{13}C(CO_2)$ in the arc-backarc hydrothermal fluids is rich in ^{13}C relative to that in the MOR hydrothermal fluids. Relative to the those in the arc-backarc hydrothermal fluids, all of the $\delta^{13}C(CO_2)$ values in the Okinawa Trough hydrothermal fluids are ^{12}C-rich. In the Hatoma hydrothermal fluids, the $\delta^{13}C(CO_2)$ values ranging from –16‰ to –3‰ belongs a group of the lowest and highest values among the Okinawa Trough hydrothermal fluids (Fig. 9). In pore water, $\delta^{13}C(CO_2)$ values are as low as –40‰ in near-surface sediments, while those are almost constant at around 0 ± 5‰ in sediments from around 100 mbsf to ~1000 mbsf (Claypool and Threlkeld, 1983; Lyon, 1973; Pisciotto and Mahoney, 1981; Schoell, 1982; Toki *et al.*, 2012). Those values are due to isotopic fractionation of microbial methanogenesis utilizing CO_2 derived from organic matter (Claypool and Kvenvolden, 1983; Galimov and Kvenvolden, 1983). But CO_2 in pore water in deeper sediment around 1000 mbsf, especially in the high thermal gradient area such as off Muroto, is derived from thermal decomposition of organic matter, $\delta^{13}C(CO_2)$ values in the pore water get close to –20‰ (Gamo *et al.*, 1993), because thermal decomposition of organic matter occur above 80°C (Quigley and Mackenzie, 1988). These CO_2 derived from thermal decomposition of organic matter is often found accompanying natural gases (Jenden *et al.*, 1988). Around hydrothermal systems, thermal decomposition would occur at shallower layers than in normal seafloor. Actually, deep-sea drilling was conducted in a sediment-covered hydrothermal field of Escanaba Trough, $\delta^{13}C(CO_2)$ values in the void gases showed around –15‰ (Ishibashi *et al.*, 2002), but $\delta^{13}C(CO_2)$ values in the vent fluids in Escanaba Trough showed around –3‰ (Ishibashi *et al.*, 2002), which is an issue of a mixing ratio. The end-member $\delta^{13}C(CO_2)$ values in the Hatoma hydrothermal fluids between –13‰ and –8‰ cannot be explained by a mixture between CO_2 in MORB, that in subducting materials, and that in pore waters, suggesting that CO_2 derived from thermal decomposition of –20‰ has no small influence on the Hatoma hydrothermal fluids (Fig.

9). This inference is supported by the chemical compositions of the hydrothermal fluids, such as their NH_4^+, I, and B concentrations. These chemical components, which are derived from organic matter decomposition, clearly influence the chemistry of the Hatoma hydrothermal fluids. It is therefore reasonable to infer that the CO_2 originates in part from organic carbon. The concentrations of CO_2 in the hydrothermal fluids at Hatoma are much higher than concentrations in MOR hydrothermal fluids (Fig. 5h). High CO_2 concentration in the Izena hydrothermal fluids are derived from the subducting slab (Ishibashi *et al*., 1995; Sakai *et al*., 1990a). This difference of the origin of CO_2 is due to the different $\delta^{13}C(CO_2)$ values in the Izena and Hatoma hydrothermal fluids; from –5.0 to –4.7‰ in the Izena fluids (Ishibashi *et al*., 1995), on the other hand from –16 to –3‰ in the Hatoma fluids (Table 2). In the Iheya fluids from –10.1 to –6.1‰, the CO_2 was mainly derived from subducting slab (Kawagucci *et al*., 2011), but they did not deny the possibility of thermogenic CO_2. Even in this study, the influence of thermogenic CO_2 is not so large, the main source of CO_2 in the Hatoma hydrothermal fluids would be a mixture of CO_2 in MORB, subducting materials, or pore water. It is noteworthy that all of the $\delta^{13}C(CO_2)$ values in the Okinawa Trough hydrothermal fluids are enriched in ^{12}C relative to the sediment-starved arc-backarc hydrothermal fluids (Fig. 9), suggesting that thermogenic CO_2 should influence on the CO_2 in the Okinawa Trough hydrothermal fluids. Next, Thermal decomposition generates also thermogenic methane, so we discuss the origin of the methane in the Hatoma hydrothermal fluids.

About methane in hydrothermal fluids, as Kawagucci *et al*. (2013b) complied very well, we can observed only μM order of methane in EPR (Welhan and Craig, 1983). Originally, methane in seawater is just only nM order, and it is not generated from MORB so much (McCollom and Seewald, 2007). The largest source of methane in hydrothermal fluids is sediment (Kawagucci *et al*., 2013b), and the generation pathway of methane in the sediments is two different processes; microbial methanogenesis or thermal decomposition of organic matter in sediments. Microbial methanogenesis occurs at a lower temperature condition than 122°C (Takai *et al*., 2008a), on the other hand, thermal decomposition of organic matter occurs at a higher temperature condition than 80°C (Quigley and Mackenzie, 1988). We have long used Bernard plots to assess the origin of methane in natural gas studies (Bernard *et al*., 1976). Recently a new method of evaluating hydrocarbons in hydrothermal systems has been proposed by Kawagucci *et al*. (2013b). Like Bernard plots, this new method also uses the relationship between carbon isotope ratios ($\delta^{13}C(CH_4)$) and the concentration ratios of light hydrocarbons ($CH_4/(C_2H_6+C_3H_8) = C_1/(C_2+C_3)$). However, the combinations of $\delta^{13}C(CH_4)$ and $C_1/(C_2+C_3)$ that indicate whether methane is of microbial or thermogenic origin differ from those of a Bernard plot. According to Kawagucci *et al*. (2013b), microbial methane $\delta^{13}C(CH_4) = -100‰$ to $-30‰$ and $C_1/(C_2+C_3) > 10^4$, whereas the corresponding values of thermogenic methane are $-30‰ < \delta^{13}C(CH_4) < -20‰$ and $10^0 < C_1/(C_2+C_3) < 10^2$.

Kawagucci *et al*. (2013b) adopted –100‰ to –30‰ for $\delta^{13}C(CH_4)$ of microbial methane based on isotopic fractionation factors from many incubation experiments and $\delta^{13}C$ of the substrates. Data from many cores of subseafloor sediments obtained by the Deep Sea Drilling Project from the world's oceans show that, except in particular environments such as near oil or gas fields, $\delta^{13}C(CH_4)$ values of hydrocarbons in near-surface sediments are around –85‰, whereas in sediments from around 100 mbsf to ~1000 mbsf, $\delta^{13}C(CH_4)$ values are almost constant at around –70‰ (Berner and Bertrand, 1991; Claypool and Threlkeld, 1983; Galimov *et al*., 1980; Lyon, 1973; Pflaum *et al*., 1986; Pisciotto and Mahoney, 1981; Schoell, 1982; Toki *et al*., 2012; Waseda and Didyk, 1995; Whiticar and Faber, 1987). Similarly, $C_1/(C_2+C_3)$ values are almost constant between 10^3 and 10^4 (Berner and Bertrand, 1991; Claypool and Threlkeld, 1983; Galimov *et al*., 1980; Pflaum *et al*., 1986; Schoell, 1982; Toki *et al*., 2012; Waseda and Didyk, 1995; Whiticar and Faber, 1987). Thus, we adopted a value of –70‰ for $\delta^{13}C(CH_4)$ and 10^3–10^4 for $C_1/(C_2+C_3)$ ratio of microbial methane.

The $\delta^{13}C(CH_4)$ value of thermogenic methane depends on the $\delta^{13}C$ value of the organic matter substrate from which it is produced. Sheu *et al*. (1999) reported $\delta^{13}C$ values of sediment to range from –25‰ to –21‰ in the East China Sea generally, but from –25‰ to –23‰ at water depths of more than 1400 m in the SOT area. Moreover, the $\delta^{13}C(CH_4)$ values of thermogenic methane generated from this sediment substrate are known to be close to the substrate value when the precursor sediment is relatively mature during a mature stage, but lower than the substrate value when the sediment is less mature (Berner and Faber, 1996). When the substrate from which thermogenic methane is generated is sediment, its maturity is moderate, as indicated by vitrinite reflectances between 0.5 and 2.0% R_o (Berner and Faber, 1996). Using an equation proposed by Berner and Faber (1996), we calculated that the $\delta^{13}C$ value of thermogenic methane generated from bulk sediment should be in the range of –32‰ to –25‰. Taking into account this range, along with the range (–25‰ to –23‰) reported by (Sheu *et al*., 1999) for the SOT area, we adopted $-32‰ < \delta^{13}C(CH_4) < -25‰$ as the range for thermogenic methane in the Okinawa Trough.

The propane end-member concentration for the Hatoma hydrothermal fluid could not be calculated; in-

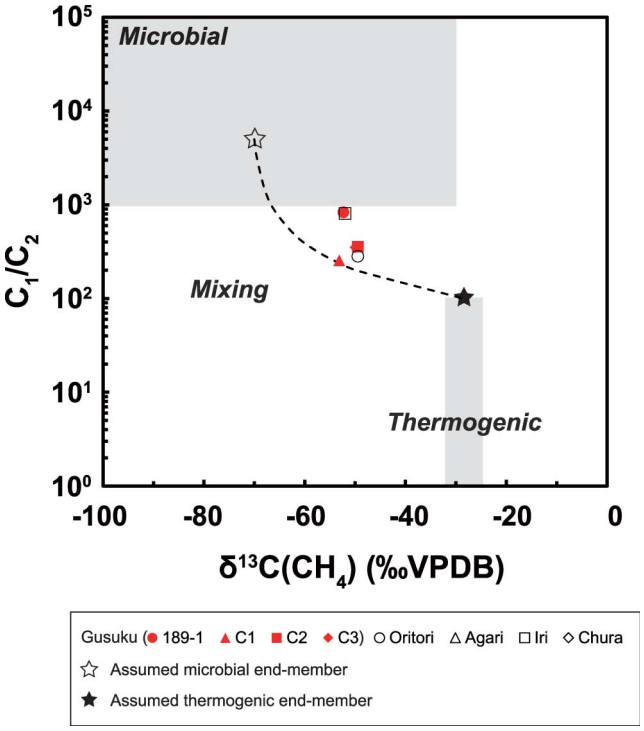

Fig. 10. Relationships between the carbon isotopic composition of methane and the C_1/C_2 ratio of volatile hydrocarbons in high-temperature fluids from the Hatoma Knoll hydrothermal system. Light gray shading shows the ranges of values attributed to microbial and thermogenic methane gas. The dashed line denotes the mixing curve between the microbial end-member (open star) and the thermogenic end-member (solid star).

stead, we calculated C_1/C_2 ratios using the endmember CH_4 and C_2H_6 concentrations (Table 2). The propane concentrations would be one digit smaller than those of ethane in the hydrothermal fluids; even if they were detected, the $C_1/(C_2+C_3)$ ratios that ideally we would like to use might be about 10% smaller than the C_1/C_2 ratios. In Fig. 10, we plotted the C_1/C_2 on a logarithmic scale, so a deviation of just 10% would be smaller than the size of the symbol. The relationship between $\delta^{13}C(CH_4)$ and C_1/C_2 ratios in the Hatoma hydrothermal fluids at each site is shown in Fig. 10 along with the assumed locations of the microbial and thermogenic end-members. The locations of the Hatoma sites in relation to the mixing line suggest that the origin of methane in the hydrothermal fluid is mostly microbial. In the MMR model, the hydrothermal system in Hatoma Knoll is classified as the Iheya North type (Kawagucci, 2015), in which microbial methane is dominant in the hydrothermal fluids. Thus, our inference that the methane at Hatoma is of mostly microbial origin is consistent with this model. We therefore conclude that the methane in the Hatoma hydrothermal fluids is a mixture of mainly microbial and a little thermogenic methane. In our data, however, the hydrocarbons of the samples are relatively CH_4-rich compared with the expected mixing line (Fig. 10). A possible explanation is that thermal decomposition occurred above 275°C (Kawagucci *et al.*, 2013b), or molecular fractionation may have occurred during the long transport of the sediment column (Fuex, 1980). Microbial methane is generated at relatively low temperatures, so our results suggest that the methane in the Hatoma hydrothermal fluid was supplied from sediments under low-temperature conditions, which is consistent with methane generated in a recharge zone of the hydrothermal system, as indicated by the MMR model. Therefore, these results are another indication that the covering sediments affect the hydrothermal chemistry at Hatoma Knoll.

Hydrothermal circulation at Hatoma Knoll

Kawagucci *et al.* (2011) have suggested that microbial methane is vented from several hydrothermal systems around the world: Endeavour, Guaymas, Middle Valley, and Iheya North. Because microbes cannot live in the discharge area, they suggested that methane in pore water in the recharge area of these hydrothermal systems enters the hydrothermal fluid. This is the "MMR model" (Microbial Methanogenesis in the Recharge area of hydrothermal circulation) (Kawagucci *et al.*, 2011). In Hatoma Knoll, the methane in the hydrothermal fluids is mostly derived from microbial production, so the Hatoma hydrothermal system is consistent with the MMR. Moreover, the $\delta^{13}C(CH_4)$ values in the Hatoma hydrothermal fluids are the lowest among the Okinawa hydrothermal fluids, and the body of Hatoma Knoll is small relative to those of other Okinawa Trough hydrothermal systems (Kawagucci, 2015). These facts indicate that, relative to the size of the Hatoma body, a large recharge zone could lead the $\delta^{13}C(CH_4)$ values to the lowest among the Okinawa fluids. Determining the scale of the recharge zone is a topic for future research of hydrothermal systems through direct drilling or newly developed imaging techniques with a high-resolution.

Conclusion

We investigated the chemical and isotopic compositions of hydrothermal fluids in Hatoma Knoll in the Southern Okinawa Trough. The concentrations of most chemical components plotted linearly, mostly along two lines, against Mg concentrations, suggesting that the chemical composition of the hydrothermal fluids can be explained as a mixture of two different pure hydrothermal fluids and seawater. Although the end-member concentrations of the chemical components, calculated by extrapolating Mg to 0 mmol/kg, indicated two source fluids, the end-member concentration ratios were mostly consistent, sug-

gesting that the hydrothermal fluids were derived from a single pure hydrothermal fluid source that underwent phase separation beneath the seafloor before venting. The end-member Cl^- concentrations were all lower than the seawater concentration, suggesting that only a vapor phase vents from the Hatoma system. The highest temperature fluid with the lowest Cl^- concentration was from vents in the vicinity of the center of the crater (at Gusuku, Oritori, and Agari), suggesting that this area is the center of hydrothermal activity. Compared to other hydrothermal fluids in the world, the Hatoma hydrothermal fluids have higher pH, alkalinity, and NH_4^+, B, K, Li, CH_4, and CO_2 concentrations, but lower Fe and Al concentrations, suggesting that they have a similar characteristics to those of the other Okinawa Trough hydrothermal fluids. The positive $\delta^{18}O$ and negative δD values of H_2O in the hydrothermal fluid suggests that the fluids are influenced by sediments or subducted-related volcanic vapors. The low $^3He/^4He$ values relative to those of the other hydrothermal fluids indicate that much of the helium was of crustal origin, including sediments. The crustal helium could have originated from the covering sediment in the Okinawa Trough or pore waters in the sediments. Based on the $\delta^{13}C$ of CO_2 in the hydrothermal fluids, the CO_2 in the hydrothermal fluids would be influenced by CO_2 derived from thermal decomposition of organic matter, but mainly from that in mantle, subducting materials, or pore waters. $\delta^{13}C(CH_4)$ values in the hydrothermal fluids indicate that most of the CH_4 was of microbial origin in the pore waters. The microbial methane contribution is higher than that in most other hydrothermal systems and comparable to that in the Iheya North system. The Hatoma Knoll hydrothermal system is an MMR type-system, meaning that microbial methanogenesis occurs in pore waters in the sediments in the recharge zone. Sediments influence all Okinawa Trough hydrothermal systems, but the Hatoma hydrothermal system $\delta^{13}C(CH_4)$ values are the lowest among these systems, suggesting that the Hatoma hydrothermal system is the most highly influenced by the sediments in the recharge zone among the Okinawa Trough hydrothermal systems. Therefore the degree of the sediment influences has a variation in the Okinawa Trough hydrothermal field.

Acknowledgments—During the sampling, we benefited from the expertise of the commander and members of the *Shinkai 2000*, the *Hyper Dolphin*, and the *Shinkai 6500* operation teams, and from that of the captains and crews of R/V *Natsushima* and R/V *Yokosuka*. This paper was modified from the master's theses of Daigo Iwata and Michihiro Itoh, so we are grateful to Professor Shigeru Ohde and Professor Tamotsu Oomori for their supervision of the work. We owe the alumnae and alumni of each laboratory for their help with the onboard analyses: Horoyuki Akashi (Yamanaka Lab), Hiroki Nakano (Ishibashi Lab), Kazuhiro Inoue (TITEC). We express our sincere gratitude to everyone associated with this work, and especially to Satomi Minamizawa from Nippon Marine Enterprises (NME) for support of the ocean research. This study was supported by a Grant-in-Aid for Scientific Research on Innovative Areas from Ministry of Education, Culture, Sports, Science and Technology (MEXT) and the TAIGA project. While writing this report, we were supported by the International Research Hub Project for Climate Change and Coral Reef/Island Dynamics at the University of the Ryukyus, and by the promotion budget of a strategic study of achievement of a medium-term plan in 2014 "Integrated geochemical study of islands and oceanic environments at the Ryukyu arc (Representative: Ryuichi Shinjo)" and "Integrated Geo-environmental Science of the Ryukyu Islands (Representative: Kazuhiko Fujita)" in 2015.

REFERENCES

Bernard, B. B., Brooks, J. M. and Sackett, W. M. (1976) Natural gas seepage in the Gulf of Mexico. *Earth Planet. Sci. Lett*. **31**, 48–54.

Berndt, M. E. and Seyfried, W. E., Jr. (1993) Calcium and sodium exchange during hydrothermal alteration of calcic plagioclase at 400°C and 400 bars. *Geochim. Cosmochim. Acta* **57**, 4445–4451.

Berner, U. and Bertrand, P. (1991) Light hydrocarbons in sediments of the Sulu Sea basin (Site 768); genetic characterization by molecular and stable isotope composition. *Proceedings of the Ocean Drilling Program* (Silver, E. A., Rangin, C., von Breymann, M. T., Berner, U., Bertrand, P., Betzler, C., Brass, G. W., Hsue, V., Huang, Z., Jarrard, R. D., Lewis, S. D., Linsley, B. K., Merrill, D. L., Mueller, C. M., Nederbragt, A. J., Nichols, G. J., Pubellier, M., Sajona, F. G., Scherer, R. P., Sheu, D. D., Shibuya, H., Shyu, J.-P., Smith, R. B., Smith, T., Solidum, R. U., Spadea, P., Tannant, D. D., Winkler, W. R., eds.), 227–231, Texas A&M University, Ocean Drilling Program, College Station.

Berner, U. and Faber, E. (1996) Empirical carbon isotope/maturity relationships for gases from algal kerogens and terrigenous organic matter, based on dry, open-system pyrolysis. *Org. Geochem*. **24**, 947–955.

Bischoff, J. L. and Dickson, F. W. (1975) Seawater-basalt interaction at 200°C and 500 bars: Implications for origin of sea-floor heavy-metal deposits and regulation of seawater chemistry. *Earth Planet. Sci. Lett*. **25**, 385–397.

Bischoff, J. L. and Pitzer, K. S. (1989) Liquid-vapor relations for the system NaCl-H_2O; summary of the P-T-x surface from 300 degrees to 500 degrees C. *Am. J. Sci*. **289**, 217–248.

Bischoff, J. L. and Rosenbauer, R. J. (1985) An empirical equation of state for hydrothermal seawater (3.2 percent NaCl). *Am. J. Sci*. **285**, 725–763.

Butterfield, D. A., Massoth, G. J., McDuff, R. E., Lupton, J. E. and Lilley, M. D. (1990) Geochemistry of hydrothermal fluids from Axial Seamount hydrothermal emissions study vent field, Juan de Fuca Ridge: Subseafloor boiling and subsequent fluid-rock interaction. *J. Geophys. Res.: Solid Earth* **95**, 12895–12921.

Butterfield, D. A., McDuff, R. E., Franklin, J. and Wheat, G. C. (1994a) Geochemistry of hydrothermal vent fluids from

Middle Valley, Juan de Fuca Ridge. *Proceedings of the Ocean Drilling Program, Scientific Results* **139**, 395–410.

Butterfield, D. A., McDuff, R. E., Mottl, M. J., Lilley, M. D., Lupton, J. E. and Massoth, G. J. (1994b) Gradients in the composition of hydrothermal fluids from the Endeavour segment vent field: Phase separation and brine loss. *J. Geophys. Res.: Solid Earth* **99**, 9561–9583.

Butterfield, D. A., Seyfried, W. E., Jr. and Lilley, M. D. (2003) Composition and evolution of hydrothermal fluids. *Energy and Mass Transfer in Marine Hydrothermal Systems* (Halbach, P., Tunnicliffe, V. and Hein, J. R., eds.), 123–161, Dahlem University Press.

Chang, Y.-P., Wu, S.-M., Wei, K.-Y., Murayama, M., Kawahata, H. and Chen, M.-T. (2005) Foraminiferal oxygen isotope stratigraphy and high-resolution organic carbon, carbonate records from the Okinawa Trough (IMAGES MD012404 and ODP Site 1202). *Terr. Atmos. Ocean. Sci*. **16**, 57–73.

Chang, Y.-P., Chen, M.-T., Yokoyama, Y., Matsuzaki, H., Thompson, W. G., Kao, S.-J. and Kawahata, H. (2009) Monsoon hydrography and productivity changes in the East China Sea during the past 100,000 years: Okinawa Trough evidence (MD012404). *Paleoceanography*, **24**, PA3208.

Charlou, J. L., Donval, J. P., Jean-Baptiste, P., Dapoigny, A. and Rona, P. A. (1996) Gases and helium isotopes in high temperature solutions sampled before and after ODP Leg 158 drilling at TAG Hydrothermal Field (26°N, MAR). *Geophys. Res. Lett*. **23**, 3491–3494.

Charlou, J. L., Donval, J. P., Fouquet, Y., Jean-Baptiste, P. and Holm, N. (2002) Geochemistry of high H_2 and CH_4 vent fluids issuing from ultramafic rocks at the Rainbow hydrothermal field (36°14′ N, MAR). *Chem. Geol*. **191**, 345–359.

Chiba, H., Nakashima, K., Gamo, T., Ishibashi, J., Tsunogai, U. and Sakai, H. (1993) Hydrothermal activity at the Minami-Ensei Knoll, Okinawa Trough: chemical characteristics of hydrothermal solutions. *Proc. JAMSTEC Symp. Deep-Sea Res*. **9**, 271–282 (in Japanese with English abstract).

Claypool, G. E. and Kvenvolden, K. A. (1983) Methane and other hydrocarbon gases in marine sediment. *Ann. Rev. Earth Planet. Sci*. **11**, 299–327.

Claypool, G. E. and Threlkeld, C. N. (1983) Anoxic diagenesis and methane generation in sediments of the Blake Outer Ridge, Deep Sea Drilling Project Site 533, Leg 76. *Initial Reports of the Deep Sea Drilling Project* (Sheridan, R. E., Gradstein, F. M. *et al*., eds.), 391–401, U.S. Govt. Printing Office.

Cline, J. D. (1969) Spectrophotometric determination of hydrogen sulfide in natural waters. *Limnol. Oceanogr*. **14**, 454–458.

Coplen, T. B., Wildman, J. D. and Chen, J. (1991) Improvements in the gaseous hydrogen-water equilibration technique for hydrogen isotope-ratio analysis. *Anal. Chem*. **63**, 910–912.

Craig, H., Lupton, J. E. and Horibe, Y. (1978) A mantle helium component in Circum-Pacific volcanic gases: Hakone, the Marianas. and Mt. Lassen. *Terrestrial Rare Gases* (Alexander, E. C. and Ozima, M., eds.), 3–16, Japan Science Society Press.

Cruse, A. M. and Seewald, J. S. (2001) Metal mobility in sediment-covered ridge-crest hydrothermal systems: experimental and theoretical constraints. *Geochim. Cosmochim. Acta* **65**, 3233–3247.

Cruse, A. M. and Seewald, J. S. (2006) Geochemistry of low-molecular weight hydrocarbons in hydrothermal fluids from Middle Valley, northern Juan de Fuca Ridge. *Geochim. Cosmochim. Acta* **70**, 2073–2092.

de Ronde, C. E. J., Massoth, G. J., Butterfield, D. A., Christenson, B. W., Ishibashi, J., Ditchburn, R. G., Hannington, M. D., Brathwaite, R. L., Lupton, J. E., Kamenetsky, V. S., Graham, I. J., Zellmer, G. F., Dziak, R. P., Embley, R. W., Dekov, V. M., Munnik, F., Lahr, J., Evans, L. J. and Takai, K. (2011) Submarine hydrothermal activity and gold-rich mineralization at Brothers Volcano, Kermadec Arc, New Zealand. *Mineral. Deposita* **46**, 541–584.

Diekmann, B., Hofmann, J., Henrich, R., Fütterer, D. K., Röhl, U. and Wei, K.-Y. (2008) Detrital sediment supply in the southern Okinawa Trough and its relation to sea-level and Kuroshio dynamics during the late Quaternary. *Mar. Geol*. **255**, 83–95.

Dolfing, J. (1988) Acetogenesis. *Biology of Anaerobic Microorganisms* (Zehnder, A. J. B., ed.), 417–468, John Wiley & Sons Inc.

Dou, Y., Yang, S., Liu, Z., Clift, P. D., Shi, X., Yu, H. and Berne, S. (2010a) Provenance discrimination of siliciclastic sediments in the middle Okinawa Trough since 30 ka: Constraints from rare earth element compositions. *Mar. Geol*. **275**, 212–220.

Dou, Y., Yang, S., Liu, Z., Clift, P. D., Yu, H., Berne, S. and Shi, X. (2010b) Clay mineral evolution in the central Okinawa Trough since 28 ka: Implications for sediment provenance and paleoenvironmental change. *Palaeogeogr. Palaeoclimatol. Palaeoecol*. **288**, 108–117.

Duan, Z. and Sun, R. (2003) An improved model calculating CO_2 solubility in pure water and aqueous NaCl solutions from 273 to 533 K and from 0 to 2000 bar. *Chem. Geol*. **193**, 257–271.

Epstein, S. and Mayeda, T. (1953) Variation of O18 content of waters from natural sources. *Geochim. Cosmochim. Acta* **4**, 213–224.

Expedition 331 Scientists (2010) Deep hot biosphere. *IODP Preliminary Report* **331**, 1–63.

Fourre, E., Jean-Baptiste, P., Charlou, J. L., Donval, J. P. and Ishibashi, J. (2006) Helium isotopic composition of hydrothermal fluids from the Manus back-arc Basin, Papua New Guinea. *Geoghem. J*. **40**, 245–252.

Foustoukos, D. I. and Seyfried, W. E. (2007) Fluid phase separation processes in submarine hydrothermal systems. *Rev. Mineral. Geochem*. **65**, 213–239.

Foustoukos, D. I. and Seyfried, W. E., Jr. (2007) Quartz solubility in the two-phase and critical region of the NaCl-KCl-H_2O system: Implications for submarine hydrothermal vent systems at 9°50′ N East Pacific Rise. *Geochim. Cosmochim. Acta* **71**, 186–201.

Fuex, A. N. (1980) Experimental evidence against an appreciable isotopic fractionation of methane during migration. *Advances in Organic Geochemistry 1979* (Douglas, A. G. and Maxwell, J. R., eds.), 725–732, Pergamon Press.

Galimov, E. M. and Kvenvolden, K. A. (1983) Concentrations

and carbon isotopic compositions of CH_4 and CO_2 in gas from sediments of the Blake Outer Ridge, Deep Sea Drilling Project Leg 76. *Initial Reports of the Deep Sea Drilling Project* (Sheridan, R. E., Gradstein, F. M. *et al*., eds.), 403–407, U.S. Govt. Printing Office.

Galimov, E. M., Chinyonov, V. A. and Ivanov, Y. N. (1980) Isotopic composition of methane carbon and the relative content of gaseous hydrocarbons in the deposits of the Moroccan Basin of the Atlantic Ocean (Deep Sea Drilling Project sites 415 and 416). (Stout, L. N., Worstell, P., Lancelot, Y., Winterer, E. L., Bosellini, A., Boutefeu, A. G., Boyce, R. E., Cepek, P., Fritz, D., Galimov, E. M., Melguen, M., Price, I., Schlager, W., Sliter, W., Taguchi, K., Vincent, E. and Westberg, J., eds.), 615–622, Texas A&M University, Ocean Drilling Program, College Station.

Gamo, T. (1995) Wide variation of chemical characteristics of submarine hydrothermal fluids due to secondary modification processes after high temperature water-rock interaction: a review. *Biogeochemical Processes and Ocean Flux in the Western Pacific* (Sakai, H. and Nozaki, Y., eds.), 425–451, Terra Scientific Publishing Company.

Gamo, T., Kastner, M., Berner, U. and Gieskes, J. (1993) Carbon isotope ratio of total inorganic carbon in pore waters associated with diagenesis of organic material at Site 808, Nankai Trough. *Proceedings of the Ocean Drilling Program, Scientific Results* (Hill, I. A., Taira, A., Firth, J. V. *et al*., eds.), 159–163, College Station.

GANSEKI (2007.10.22) Deep Seafloo Rock Sample Database.

Gieskes, J. M., Gamo, T. and Brumsack, H. (1991) Chemical methods for interstitial water analysis aboard JOIDES Resolution. *Ocean Drilling Program Texas A&M University Technical Note* **15**, 1–60.

Giggenbach, W. F. (1992) Isotopic shifts in waters from geothermal and volcanic systems along convergent plate boundaries and their origin. *Earth Planet. Sci. Lett*. **113**, 495–510.

Glasby, G. P. and Notsu, K. (2003) Submarine hydrothermal mineralization in the Okinawa Trough, SW of Japan: an overview. *Ore Geol. Rev*. **23**, 299–339.

Hajash, A. and Chandler, G. W. (1982) An experimental investigation of high-temperature interactions between seawater and rhyolite, andesite, basalt and peridotite. *Contrib Mineral Petrol*. **78**, 240–254.

Hannington, M., Herzig, P., Stoffers, P., Scholten, J., Botz, R., Garbe-Schönberg, D., Jonasson, I. R. and Roest, W. (2001) First observations of high-temperature submarine hydrothermal vents and massive anhydrite deposits off the north coast of Iceland. *Mar. Geol*. **177**, 199–220.

Hanzawa, S. (1935) Topography and geology of the Ryukyu Islands. *Tohoku University Science Report 2nd Series (Geology)* **17**, 1–61.

Hedenquist, J. W. and Lowenstern, J. B. (1994) The role of magmas in the formation of hydrothermal ore deposits. *Nature* **370**, 519–527.

Honda, M. C., Kusakabe, M., Nakabayashi, S., Manganini, S. and Honjo, S. (1997) Change in pCO_2 through biological activity in the marginal seas of the western North Pacific—The efficiency of the biological pump estimated by a sediment trap experiment—. *J. Oceanogr*. **53**, 645–662.

Hung, J. J., Lin, C. S., Chung, Y. C., Hung, G. W. and Liu, W. S. (2003) Lateral fluxes of biogenic particles through the Mien-Hua canyon in the southern East China Sea slope. *Cont. Shelf Res*. **23**, 935–955.

Inagaki, F., Kuypers, M. M. M., Tsunogai, U., Ishibashi, J., Nakamura, K., Treude, T., Ohkubo, S., Nakaseama, M., Gena, K., Chiba, H., Hirayama, H., Nunoura, T., Takai, K., Jørgensen, B. B., Horikoshi, K. and Boetius, A. (2006) Microbial community in a sediment-hosted CO_2 lake of the southern Okinawa Trough hydrothermal system. *Proc. Nat. Acad. Sci*. **103**, 14164–14169.

Ishibashi, J., Wakita, H., Nojiri, Y., Grimaud, D., Jean-Baptiste, P., Gamo, T., Auzende, J.-M. and Urabe, T. (1994) Helium and carbon geochemistry of hydrothermal fluids from the North Fiji Basin spreading ridge (southwest Pacific). *Earth Planet. Sci. Lett*. **128**, 183–197.

Ishibashi, J., Sano, Y., Wakita, H., Gamo, T., Tsutsumi, M. and Sakai, H. (1995) Helium and carbon geochemistry of hydrothermal fluids from the Mid-Okinawa Trough Back Arc Basin, southwest of Japan. *Chem. Geol*. **123**, 1–15.

Ishibashi, J., Sato, M., Sano, Y., Wakita, H., Gamo, T. and Shanks Iii, W. C. (2002) Helium and carbon gas geochemistry of pore fluids from the sediment-rich hydrothermal system in Escanaba Trough. *Appl. Geochem*. **17**, 1457–1466.

Ishibashi, J., Nakaseama, M., Seguchi, M., Yamashita, T., Doi, S., Sakamoto, T., Shimada, K., Shimada, N., Noguchi, T., Oomori, T., Kusakabe, M. and Yamanaka, T. (2008) Marine shallow-water hydrothermal activity and mineralization at the Wakamiko crater in Kagoshima bay, south Kyushu, Japan. *J. Volcanol. Geotherm. Res*. **173**, 84–98.

Ishibashi, J., Noguchi, T., Toki, T., Miyabe, S., Yamagami, S., Onishi, Y., Yamanaka, T., Yokoyama, Y., Omori, R., Takahashi, Y., Hatada, K., Nakaguchi, J., Yoshizaki, M., Konno, Y., Shibuya, T., Takai, K., Inagaki, F. and Kawagucci, S. (2014) Diversity of fluid geochemistry affected by processes during fluid upwelling in active hydrothermal fields in the Izena Hole, the middle Okinawa Trough back-arc basin. *Geochem. J*. **48**, 357–369.

Ishibashi, J., Tsunogai, U., Toki, T., Ebina, N., Gamo, T., Sano, Y., Masuda, H. and Chiba, H. (2015) Chemical composition of hydrothermal fluids in the central and southern Mariana Trough backarc basin. *Deep-Sea Res. Part II: Topical Studies in Oceanography* **121**, 126–136.

Itai, T. and Kusakabe, M. (2004) Some practical aspects of an on-line chromium reduction method for D/H analysis of natural waters using a conventional IRMS. *Geochem. J*. **38**, 435–440.

Jenden, P. D., Kaplan, I. R., Poreda, R. and Craig, H. (1988) Origin of nitrogen-rich natural gases in the California Great Valley: Evidence from helium, carbon and nitrogen isotope ratios. *Geochim. Cosmochim. Acta* **52**, 851–861.

Kawagucci, S. (2015) Fluid geochemistry of high-temperature hydrothermal fields in the Okinawa Trough: How and where TAIGA of Methane is generated. *Subseafloor Biosphere Linked to Global Hydrothermal Systems; TAIGA Concept 30* (Okino, K., Ishibashi, J. and Sunamura, M., eds.), 387–403, Springer.

Kawagucci, S., Chiba, H., Ishibashi, J., Yamanaka, T., Toki, T.,

Muramatsu, Y., Ueno, Y., Makabe, A., Inoue, K., Yoshida, N., Nakagawa, S., Nunoura, T., Takai, K., Takahata, N., Sano, Y., Narita, T., Teranishi, G., Obata, H. and Gamo, T. (2011) Hydrothermal fluid geochemistry at the Iheya North field in the mid-Okinawa Trough: Implication for origin of methane in subseafloor fluid circulation systems. *Geochem. J.* **45**, 109–124.

Kawagucci, S., Miyazaki, J., Nakajima, R., Nozaki, T., Takaya, Y., Kato, Y., Shibuya, T., Konno, U., Nakaguchi, Y., Hatada, K., Hirayama, H., Fujikura, K., Furushima, Y., Yamamoto, H., Watsuji, T., Ishibashi, J. and Takai, K. (2013a) Post-drilling changes in fluid discharge pattern, mineral deposition, and fluid chemistry in the Iheya North hydrothermal field, Okinawa Trough. *Geochem., Geophys., Geosyst.* **14**, 4774–4790.

Kawagucci, S., Ueno, Y., Takai, K., Toki, T., Ito, M., Inoue, K., Makabe, A., Yoshida, N., Muramatsu, Y., Takahata, N., Sano, Y., Narita, T., Teranishi, G., Obata, H., Nakagawa, S., Nunoura, T. and Gamo, T. (2013b) Geochemical origin of hydrothermal fluid methane in sediment-associated fields and its relevance to the geographical distribution of whole hydrothermal circulation. *Chem. Geol.* **339**, 213–225.

Keeling, C. D. (1961) The concentration and isotopic abundances of carbon dioxide in rural and marine air. *Geochim. Cosmochim. Acta* **24**, 277–298.

Konno, U., Tsunogai, U., Nakagawa, F., Nakaseama, M., Ishibashi, J., Nunoura, T. and Nakamura, K. (2006) Liquid CO_2 venting on seafloor: Yonaguni IV Knoll hydrothermal system, Okinawa Trough. *Geophys. Res. Lett.* **33**, L16607.

Kumagai, H., Nakamura, K., Toki, T., Morishita, T., Okino, K., Ishibashi, J., Tsunogai, U., Kawagucci, S., Gamo, T., Shibuya, T., Sawaguchi, T., Neo, N., Joshima, M., Sato, T. and Takai, K. (2008) Geological background of the Kairei and Edmond hydrothermal fields along the Central Indian Ridge: Implications of their vent fluids' distinct chemistry. *Geofluids* **8**, 239–251.

Lee, C.-S., Shor, G. G., Jr., Bibee, L. D., Lu, R. S. and Hilde, T. W. C. (1980) Okinawa Trough: Origin of a back-arc basin. *Mar. Geol.* **35**, 219–241.

Letouzey, J. and Kimura, M. (1986) The Okinawa Trough: Genesis of a back-arc basin developing along a continental margin. *Tectonophysics* **125**, 209–230.

Lilley, M. D., Butterfield, D. A., Olson, E. J., Lupton, J. E., Macko, S. A. and McDuff, R. E. (1993) Anomalous CH_4 and NH_4^+ concentrations at an unsedimented mid-ocean-ridge hydrothermal system. *Nature* **364**, 45–47.

Lupton, J., Lilley, M., Butterfield, D., Evans, L., Embley, R., Massoth, G., Christenson, B., Nakamura, K. and Schmidt, M. (2008) Venting of a separate CO_2-rich gas phase from submarine arc volcanoes: Examples from the Mariana and Tonga-Kermadec arcs. *J. Geophys. Res.: Solid Earth* **113**, B08S12.

Lyon, G. L. (1973) Interstitial water studies, Leg 15: Chemical and isotopic composition of gases from Cariaco Trench sediments. *Initial Reports of the Deep Sea Drilling Project* (Heezen, B. C., MacGregor, I. D., Foreman, H. P., Forristall, G. Z., Hekel, H., Hesse, R., Hoskins, R. H., Jones, E. J. W., Krasheninnikov, V., Okada, H., Ruef, M. H., Kaneps, A. G., eds.), 773–774, Texas A&M University, Ocean Drilling Program, College Station.

Massoth, G. J., Butterfield, D. A., Lupton, J. E., McDuff, R. E., Lilley, M. D. and Jonasson, I. R. (1989) Submarine venting of phase-separated hydrothermal fluids at Axial Volcano, Juan de Fuca Ridge. *Nature* **340**, 702–705.

Matsumoto, T., Kinoshita, M., Nakamura, M., Sibuet, J.-C., Lee, C.-S., Hsu, S.-K., Oomori, T., Shinjo, R., Hashimoto, Y., Hosoya, S., Imamura, M., Ito, M., Tukuda, K., Yagi, H., Tatekawa, K., Kagaya, I., Hokakubo, S., Okada, T. and Kimura, M. (2001) Volcanic and hydrothermal activities and possible "segmentation" of the axial rifting in the westernmost part of the Okinawa Trough—preliminary results from the YOKOSUKA/SHINKAI 6500 Lequios Cruise—. *JAMSTEC J. Deep-Sea Res.* **19**, 95–107.

McCollom, T. M. (2008) Observational, experimental, and theoretical constraints on carbon cycling in mid-ocean ridge hydrothermal systems. *Magma to Microbe: Modeling Hydrothermal Processes at Ocean Spreading Centers*, 193–213, AGU.

McCollom, T. M. and Seewald, J. S. (2007) Abiotic synthesis of organic compounds in deep-sea hydrothermal environments. *Chem. Rev.* **107**, 382–401.

Melson, W. G., Vallier, T. L., Wright, T. L., Byerly, G. and Nelen, J. (2013) Chemical diversity of abyssal volcanic glass erupted along Pacific, Atlantic, and Indian Ocean sea-floor spreading centers. *The Geophysics of the Pacific Ocean Basin and Its Margin*, 351–367, AGU.

Metz, S. and Trefry, J. H. (2000) Chemical and mineralogical influences on concentrations of trace metals in hydrothermal fluids. *Geochim. Cosmochim. Acta* **64**, 2267–2279.

Motojima, K. and Makino, T. (1965) Natural gas resources in the Ryukyu Islands. *Bull. Geol. Surv. Japan* **16**, 193–216 (in Japanese with English abstract).

Mottl, M. J. and Holland, H. D. (1978) Chemical exchange during hydrothermal alteration of basalt by seawater—I. Experimental results for major and minor components of seawater. *Geochim. Cosmochim. Acta* **42**, 1103–1115.

Mottl, M. J., Seewald, J. S., Wheat, C. G., Tivey, M. K., Michael, P. J., Proskurowski, G., McCollom, T. M., Reeves, E., Sharkey, J., You, C. F., Chan, L. H. and Pichler, T. (2011) Chemistry of hot springs along the Eastern Lau Spreading Center. *Geochim. Cosmochim. Acta* **75**, 1013–1038.

Muramatsu, Y., Doi, T., Tomaru, H., Fehn, U., Takeuchi, R. and Matsumoto, R. (2007) Halogen concentrations in pore waters and sediments of the Nankai Trough, Japan: Implications for the origin of gas hydrates. *Appl. Geochem.* **22**, 534–556.

Nakagawa, H. and Murakami, M. (1975) Geology of Kumejima, Okinawa Gunto, Ryukyu Island. *Tohoku University, Institution of Geological Paleontology, Contribution*, 1–16 (in Japanese with English abstract).

Nakano, A., Matsumura, M. and Ishibashi, J. (2001) Geochemistry of hydrothermal fluids from the Hatoma Knoll in the South Okinawa Trough. *JAMSTEC J. Deep-Sea Res.* **18**, 139–144 (in Japanese with English abstract).

Natori, H. (1976) Planktonic foraminiferal biostratigraphy and datum planes in the Late Cenozoic sedimentary sequence in Okinawa-jima, Japan. *Progress in Micropaleontology, Special Publication of Micropaleontology Press*

(Takayanagi, Y. and Saito, T., eds.), 214–243, American Museum of Natural History, Micropaleontology Press.

Obata, H., Nozaki, Y., Okamura, K., Maruo, M. and Nakayama, E. (2000) Flow-through analysis of Al in seawater by fluorometric detection with the use of lumogallion. *Field Anal. Chem. Technol*. **4**, 274–282.

Ogawa, Y., Shikazono, N., Ishiyama, D., Sato, H. and Mizuta, T. (2005) An experimental study on felsic rock-artificial seawater interaction: implications for hydrothermal alteration and sulfate formation in the Kuroko mining area of Japan. *Mineral. Deposita* **39**, 813–821.

Ohmoto, H. (1986) Stable isotope geochemistry of ore deposits. *Rev. Mineral. Geochem*. **16**, 491–559.

Okamoto, K., Ishibashi, J., Motomura, Y., Yamanaka, T. and Fujikura, K. (2002) Mineralogical Studies of Hydrothermal Deposits collected from the Dai-Yon Yonaguni Knoll and the Hatoma Knoll in the Okinawa Trough. *JAMSTEC J. Deep-Sea Res*. **21**, 75–81 (in Japanese with English abstract).

Pezzopane, S. K. and Wesnousky, S. G. (1989) Large earthquakes and crustal deformation near Taiwan. *J. Geophys. Res.: Solid Earth* **94**, 7250–7264.

Pflaum, R. C., Brooks, J. M., Cox, H. B., Kennicutt, M. C. and Sheu, D.-D. (1986) Molecular and isotopic analysis of core gases and gas hydrates, Deep Sea Drilling Project Leg 96. *Initial Reports of the Deep Sea Drilling Project* (Bouma, A. H., Coleman, J. M., Meyer, A. W. *et al*., eds.), 781–784, U.S. Govt. Printing Office.

Pisciotto, K. A. and Mahoney, J. J. (1981) Isotopic survey of diagenetic carbonates, Deep Sea Drilling Project, Leg 63. *Initial Reports of the Deep Sea Drilling Project* (Yeats, R. S., Haq, B. U. *et al*. eds.), 595–609, U.S. Govt. Printing Office.

Proskurowski, G., Lilley, M. D., Kelley, D. S. and Olson, E. J. (2006) Low temperature volatile production at the Lost City Hydrothermal Field, evidence from a hydrogen stable isotope geothermometer. *Chem. Geol*. **229**, 331–343.

Quigley, T. M. and Mackenzie, A. S. (1988) The temperatures of oil and gas formation in the sub-surface. *Nature* **333**, 549–552.

Reeves, E. P., Seewald, J. S., Saccocia, P., Bach, W., Craddock, P. R., Shanks, W. C., Sylva, S. P., Walsh, E., Pichler, T. and Rosner, M. (2011) Geochemistry of hydrothermal fluids from the PACMANUS, Northeast Pual and Vienna Woods hydrothermal fields, Manus Basin, Papua New Guinea. *Geochim. Cosmochim. Acta* **75**, 1088–1123.

Saegusa, S., Tsunogai, U., Nakagawa, F. and Kaneko, S. (2006) Development of a multibottle gas-tight fluid sampler WHATS II for Japanese submersibles/ROVs. *Geofluids* **6**, 234–240.

Sakai, H., Gamo, T., Kim, E. S., Tsutsumi, M., Tanaka, T., Ishibashi, J., Wakita, H., Yamano, M. and Oomori, T. (1990a) Venting of carbon dioxide-rich fluid and hydrate formation in mid-Okinawa Trough backarc basin. *Science* **248**, 1093–1096.

Sakai, H., Gamo, T., Kim, E. S., Shitashima, K., Yanagisawa, F., Tsutsumi, M., Ishibashi, J., Sano, Y., Wakita, H., Tanaka, T., Matsumoto, T., Naganuma, T. and Mitsuzawa, K. (1990b) Unique chemistry of the hydrothermal solution in the Mid-okinawa Trough backarc basin. *Geophys. Res. Lett*. **17**, 2133–2136.

Sano, Y. and Fischer, T. P. (2013) The analysis and interpretation of noble gases in modern hydrothermal systems. *The Noble Gases as Geochemical Tracers 10* (Burnard, P., ed.), 249–317, Springer Berlin Heidelberg.

Sano, Y. and Wakita, H. (1988) Precise measurement of helium isotopes in terrestrial gases. *Bull. Chem. Soc. Japan* **61**, 1153–1157.

Sano, Y., Takahata, N. and Seno, T. (2006) Geographical distribution of $^{3}He/^{4}He$ ratios in the Chugoku district, southwestern Japan. *Pure Appl. Geophys*. **163**, 745–757.

Schoell, M. (1982) Stable isotopic analyses of interstitial gases in quaternary sediments from the Gulf of California. *Initial Reports of the Deep Sea Drilling Project* (Curray, J. R., Moore, D. G. *et al*., eds.), 815–817, U.S. Govt. Printing Office.

Seyfried, W. E., Jr. and Bischoff, J. L. (1981) Experimental seawater-basalt interaction at 300°C, 500 bars, chemical exchange, secondary mineral formation and implications for the transport of heavy metals. *Geochim. Cosmochim. Acta* **45**, 135–147.

Seyfried, W. E., Jr. and Ding, K. (1995) Phase equilibria in seafloor hydrothermal systems: a review of the role of redox, temperature, pH and dissolved Cl on the chemistry of hot spring fluids at mid-ocean ridges. *Seafloor Hydrothermal Systems: Physical, Chemical, Biological, and Geological Interactions*, 248–272, AGU.

Seyfried, W. E., Jr., Ding, K. and Berndt, M. E. (1991) Phase equilibria constraints on the chemistry of hot spring fluids at mid-ocean ridges. *Geochim. Cosmochim. Acta* **55**, 3559–3580.

Shanks, W. C. (2001) Stable isotopes in seafloor hydrothermal systems: Vent fluids, hydrothermal deposits, hydrothermal alteration, and microbial processes. *Rev. Mineral. Geochem*. **43**, 469–525.

Shanks, W. C., III, Böhlke, J. K. and Seal, R. R., II (1995) Stable isotopes in mid-ocean ridge hydrothermal systems: Interactions between fluids, minerals, and organisms. *Seafloor Hydrothermal Systems: Physical, Chemical, Biological, and Geological Interactions*, 194–221, AGU.

Sheu, D. D., Jou, W. C., Chung, Y. C., Tang, T. Y. and Hung, J. J. (1999) Geochemical and carbon isotopic characterization of particles collected in sediment traps from the East China Sea continental slope and the Okinawa Trough northeast of Taiwan. *Cont. Shelf Res*. **19**, 183–203.

Shinjo, R. and Kato, Y. (2000) Geochemical constraints on the origin of bimodal magmatism at the Okinawa Trough, an incipient back-arc basin. *Lithos* **54**, 117–137.

Shinjo, R., Chung, S.-L., Kato, Y. and Kimura, M. (1999) Geochemical and Sr-Nd isotopic characteristics of volcanic rocks from the Okinawa Trough and Ryukyu Arc: Implications for the evolution of a young, intracontinental back arc basin. *J. Geophys. Res.: Solid Earth* **104**, 10591–10608.

Shipboard Scientific Party (2002) Site 1202. *Proceedings of the Ocean Drilling Program, Initial Report* (Salisbury, M. H., Shinohara, M., Richter, C. *et al*., eds.), 1–46, College Station.

Shiraki, R., Sakai, H., Endoh, M. and Kishima, N. (1987) Ex-

perimental studies on rhyolite- and andesite-seawater interactions at 300°C and 1000 bars. *Geochem. J.* **21**, 139–148.

Sibuet, J.-C., Letouzey, J., Barbier, F., Charvet, J., Foucher, J.-P., Hilde, T. W. C., Kimura, M., Chiao, L.-Y., Marsset, B., Muller, C. and Stéphan, J.-F. (1987) Back arc extension in the Okinawa Trough. *J. Geophys. Res.: Solid Earth* **92**, 14041–14063.

Stoffers, P., Worthington, T. J., Schwarz-Schampera, U., Hannington, M. D., Massoth, G. J., Hekinian, R., Schmidt, M., Lundsten, L. J., Evans, L. J., Vaiomo'unga, R. and Kerby, T. (2006) Submarine volcanoes and high-temperature hydrothermal venting on the Tonga arc, southwest Pacific. *Geology* **34**, 453–456.

Suzuki, R., Ishibashi, J., Nakaseama, M., Konno, U., Tsunogai, U., Gena, K. and Chiba, H. (2008) Diverse range of mineralization induced by phase separation of hydrothermal fluid: case study of the Yonaguni Knoll IV hydrothermal field in the Okinawa Trough back-arc basin. *Resour. Geol.* **58**, 267–288.

Suzuki, T. and Sato, Y. (1977) Heavy minerals in the Neogene Shimajiri Gourp, Miyako Island, Okinawa. *Bull. Geol. Surv. Japan* **28**, 569–574 (in Japanese with English abstract).

Takai, K., Nakamura, K., Toki, T., Tsunogai, U., Miyazaki, M., Miyazaki, J., Hirayama, H., Nakagawa, S., Nunoura, T. and Horikoshi, K. (2008a) Cell proliferation at 122°C and isotopically heavy CH_4 production by a hyperthermophilic methanogen under high-pressure cultivation. *Proc. Nat. Acad. Sci.* **105**, 10949–10954.

Takai, K., Nunoura, T., Ishibashi, J., Lupton, J., Suzuki, R., Hamasaki, H., Ueno, Y., Kawagucci, S., Gamo, T., Suzuki, Y., Hirayama, H. and Horikoshi, K. (2008b) Variability in the microbial communities and hydrothermal fluid chemistry at the newly discovered Mariner hydrothermal field, southern Lau Basin. *J. Geophys. Res.-Biogeosci.* **113**.

Takai, K., Nunoura, T., Horikoshi, K., Shibuya, T., Nakamura, K., Suzuki, Y., Stott, M., Massoth, G. J., Christenson, B. W., de Ronde, C. E. J., Butterfield, D. A., Ishibashi, J., Lupton, J. E. and Evans, L. J. (2009) Variability in microbial communities in black smoker chimneys at the NW Caldera Vent Field, Brothers Volcano, Kermadec Arc. *Geomicrobiol. J.* **26**, 552–569.

Takenouchi, S. and Kennedy, G. C. (1964) The binary system H_2O-CO_2 at high temperatures and pressures. *Am. J. Sci.* **262**, 1055–1074.

Taylor, H. P. (1979) Oxygen and hydrogen isotope relationships in hydrothermal ore deposits. *Geochemistry of Hydrothermal Ore Deposits* (Barnes, H. L., ed.), 236–277, Wiley.

Toki, T., Uehara, Y., Kinjo, K., Ijiri, A., Tsunogai, U., Tomaru, H. and Ashi, J. (2012) Methane production and accumulation in the Nankai accretionary prism: Results from IODP Expeditions 315 and 316. *Geochem. J.* **46**, 89–106.

Toki, T., Ishibashi, J., Noguchi, T., Tawata, M., Tsunogai, U., Yamanaka, T. and Nakamura, K. (2015) Chemical and isotopic compositions of hydrothermal fluids at Snail, Archaean, Pika, and Urashima sites in the Southern Mariana Trough. *Subseafloor Biosphere Linked to Global Hydrothermal Systems; TAIGA Concept 45* (Okino, K., Ishibashi, J. and Sunamura, M., eds.), 587–602, Springer.

Tsuburaya, H. and Sato, T. (1985) Petroleum exploration well Miyakojima-Oki. *J. Japanese Assoc. Petrol. Technol.* **50**, 25–33 (in Japanese).

Tsunogai, U., Ishibashi, J., Wakita, H., Gamo, T., Watanabe, K., Kajimura, T., Kanayama, S. and Sakai, H. (1994) Peculiar features of Suiyo Seamount hydrothermal fluids, Izu-Bonin Arc: Differences from subaerial volcanism. *Earth Planet. Sci. Lett.* **126**, 289–301.

Tsunogai, U., Yoshida, N., Ishibashi, J. and Gamo, T. (2000) Carbon isotopic distribution of methane in deep-sea hydrothermal plume, Myojin Knoll Caldera, Izu-Bonin arc: implications for microbial methane oxidation in the oceans and applications to heat flux estimation. *Geochim. Cosmochim. Acta* **64**, 2439–2452.

Tsunogai, U., Toki, T., Nakayama, N., Gamo, T., Kato, H. and Kaneko, S. (2003) WHATS: a new multi-bottle gas-tight sampler for sea-floor vent fluids. *Chikyukagaku* (*Geochemistry*) **37**, 101–109 (in Japanese with English abstract).

Von Damm, K. L. (1995) Controls on the chemistry and temporal variability of seafloor hydrothermal fluids. *Seafloor Hydrothermal Systems: Physical, Chemical, Biological, and Geological Interactions* (Humphris, S. E., Zierenberg, R. A., Mullineaux, L. S. and Thomson, R. E., eds.), 222–247, AGU.

Von Damm, K. L., Edmond, J. M., Measures, C. I. and Grant, B. (1985a) Chemistry of submarine hydrothermal solutions at Guaymas Basin, Gulf of California. *Geochim. Cosmochim. Acta* **49**, 2221–2237.

Von Damm, K. L., Edmond, J. M., Grant, B., Measures, C. I., Walden, B. and Weiss, R. F. (1985b) Chemistry of submarine hydrothermal solutions at 21°N, East Pacific Rise. *Geochim. Cosmochim. Acta* **49**, 2197–2220.

Von Damm, K. L., Bischoff, J. L. and Rosenbauer, R. J. (1991) Quartz solubility in hydrothermal seawater; an experimental study and equation describing quartz solubility for up to 0.5 M NaCl solutions. *Am. J. Sci.* **291**, 977–1007.

Von Damm, K. L., Parker, C. M., Gallant, R. M., Loveless, J. P. and The AdVenture 9 Science Party (2002) Chemical evolution of hydrothermal fluids from EPR 21°N: 23 years later in a phase separating world. *EOS Trans. AGU Fall Meeting Suppl.* **83**, Abstract V61B-1365.

Von Damm, K. L., Parker, C. M., Zierenberg, R. A., Lilley, M. D., Olson, E. J., Clague, D. A. and McClain, J. S. (2005) The Escanaba Trough, Gorda Ridge hydrothermal system: Temporal stability and subseafloor complexity. *Geochim. Cosmochim. Acta* **69**, 4971–4984.

Waseda, A. and Didyk, B. M. (1995) Isotope compositions of gases in sediments from the Chile continental margin. *Proceedings of the Ocean Drilling Program, Scientific Results* (Lewis, S. D., Behrmann, J. H., Musgrave, R. J. and Candy, S. C., eds.), 307–312, Ocean Drilling Program.

Watanabe, K. (1999) Hydrothermal activity on the Hatoma Knoll in the southern Okinawa Trough. *Proc. JAMSTEC Symp. Deep-Sea Res.*, 29–30 (in Japanese).

Watanabe, K. (2000) Dive surveys on knolls off the north-east of the Iriomote Island.—The Iriomote Knoll and the Daiichi and Daini Kohama Knolls—. *JAMSTEC J. Deep-Sea Res.* **16**, 19–28 (in Japanese with English abstract).

Watanabe, K. (2001) Mapping the hydrothermal activity area on the Hatoma Knoll in the southern Okinawa Trough. *JAMSTEC J. Deep-Sea Res*. **19**, 87–94.

Welhan, J. A. and Craig, H. (1983) Methane, Hydrogen and Helium in Hydrothermal Fluids at 21°N on the East Pacific Rise. *Hydrothermal Processes at Seafloor Spreading Centers 17* (Rona, P., Boström, K., Laubier, L. and Smith, K., Jr., eds.), 391–409, Springer US.

Welhan, J. A. and Lupton, J. E. (1987) Light hydrocarbon gases in Guaymas basin hydrothermal fluids: thermogenic versus abiogenic origin. *Am. Assoc. Petrol. Geol. Bull*. **71**, 215–223.

Whiticar, M. J. and Faber, E. (1987) Carbon and hydrogen isotopes in gas samples from Leg 95, Holes 603D and 613. *Initial Reports of the Deep Sea Drilling Project* (Poag, C. W., Watts, A. B. *et al*., eds.), 647–650, U.S. Govt. Printing Office.

Xu, Z., Li, T., Chang, F., Wan, S., Choi, J. and Lim, D. (2014) Clay-sized sediment provenance change in the northern Okinawa Trough since 22 kyr BP and its paleoenvironmental implication. *Palaeogeogr. Palaeoclimatol. Palaeoecol*. **399**, 236–245.

You, C. F., Butterfield, D. A., Spivack, A. J., Gieskes, J. M., Gamo, T. and Campbell, A. J. (1994) Boron and halide systematics in submarine hydrothermal systems: Effects of phase separation and sedimentary contributions. *Earth Planet. Sci. Lett*. **123**, 227–238.